Accepted Manuscript

Highly fluorescent and HDAC6 selective scriptaid analogues

Cassandra L. Fleming, Anthony Natoli, Jeannette Schreuders, Mark Devlin, Prusothman Yoganantharajah, Yann Gibert, Kathryn G. Leslie, Elizabeth J. New, Trent D. Ashton, Frederick M. Pfeffer

PII: S0223-5234(18)30978-4

DOI: https://doi.org/10.1016/j.ejmech.2018.11.020

Reference: EJMECH 10877

To appear in: *European Journal of Medicinal Chemistry*

Received Date: 15 August 2018

Revised Date: 28 October 2018

Accepted Date: 8 November 2018

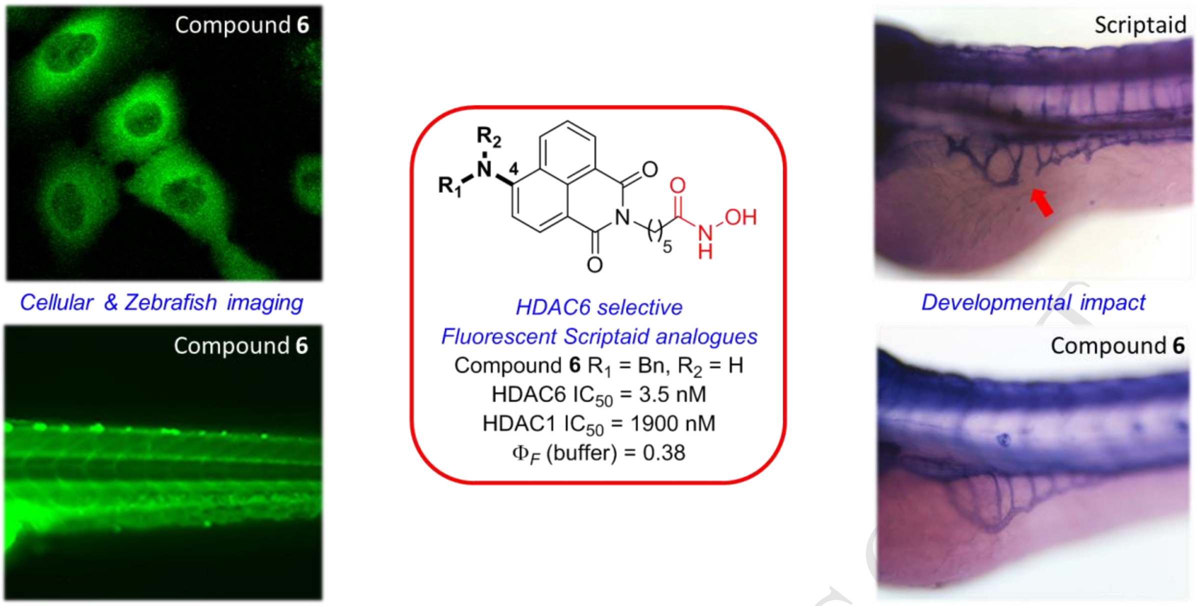
Compound 6
Cellular & Zebrafish imaging
Compound 6
HDAC6 selective
Fluorescent Scriptaid analogues
Compound 6 R_1 = Bn, R_2 = H
HDAC6 IC_{50} = 3.5 nM
HDAC1 IC_{50} = 1900 nM
Φ_F (buffer) = 0.38
Scriptaid
Developmental impact
Compound 6

Highly Fluorescent and HDAC6 Selective Scriptaid Analogues

Cassandra L. Fleming,[a] Anthony Natoli,[b] Jeannette Schreuders,[b] Mark Devlin,[b] Prusothman Yoganantharajah,[c] Yann Gibert,[c] Kathryn G. Leslie,[d] Elizabeth J. New,[d] Trent D. Ashton,[a,e,f] and Frederick M. Pfeffer[a]*

[a] School of Life & Environmental Sciences, Deakin University, Waurn Ponds, Victoria, 3216, Australia.

[b] Peter MacCallum Cancer Centre, Parkville, Melbourne, Victoria, 3000, Australia.

[c] School of Medicine, Deakin University, Waurn Ponds, Victoria, 3216, Australia.

[d] School of Chemistry, The University of Sydney, Sydney, New South Wales, 2006, Australia.

[e] Walter and Eliza Hall Institute of Medical Research, Parkville, Victoria, 3052, Australia.

[f] Department of Medical Biology, The University of Melbourne, Parkville, Victoria, 3010, Australia.

Keywords

Naphthalimide; Fluorescence; Imaging; Zebrafish; Scriptaid; 4MS, HDAC

Abstract

Fluorescent scriptaid analogues with excellent HDAC6 selectivity (HDAC1/6 > 500) and potency (HDAC6 IC_{50} < 5 nM) have been synthesised and evaluated. The highly fluorescent nature of the compounds (up to Φ_F = 0.83 in DMSO and 0.38 in aqueous buffer) makes them ideally suited for cellular imaging and visualisation of their cytoplasmic localisation was readily accomplished. Whole organism imaging in zebrafish confirmed both the vascular localisation of the new inhibitors and the impact of HDAC6 inhibition on *in vivo* development.

1 INTRODUCTION

Given their important physiological roles, members of the histone deacetylase (HDAC) family are attractive targets for therapeutic intervention,[1-6] with four HDAC inhibitors (HDACi)—vorinostat (2006, Zolinza®),[7] romidepsin (2009, Istodax®),[8] belinostat (2014, Belodaq®)[9] and panobinostat (2015, Farydak®)[10]— FDA-approved to date for the treatment of peripheral T-cell lymphoma (PTCL) and multiple myeloma. In addition, chidamide (2015, Epidaza®)[11] has been approved for use in China.

Recent concerns regarding the off-target effects associated with non-isoform-selective (pan) inhibitors have spurred efforts towards agents that are selective amongst the 18 HDAC isoforms, in particular those that target HDAC6.[2, 12-14] This class IIb isoform is located primarily in the cytoplasm and has demonstrated roles including α-tubulin deacetylation and the regulation of cytoskeletal dynamics.[1, 13, 15-19] Like other isoforms HDAC6 is clearly linked to cancer progression, however, its phenotype is unique in that mice with HDAC6 deletion are viable.[20] As such targeting HDAC6 represents a potentially less cytotoxic avenue to cancer treatment,[21] a strategy that has been shown to have merit in a melanoma xenograft mouse model.[22] As such, the design and synthesis of HDAC6 selective inhibitors has become an important pursuit (examples shown in Figure 1).[16, 21, 23-30]

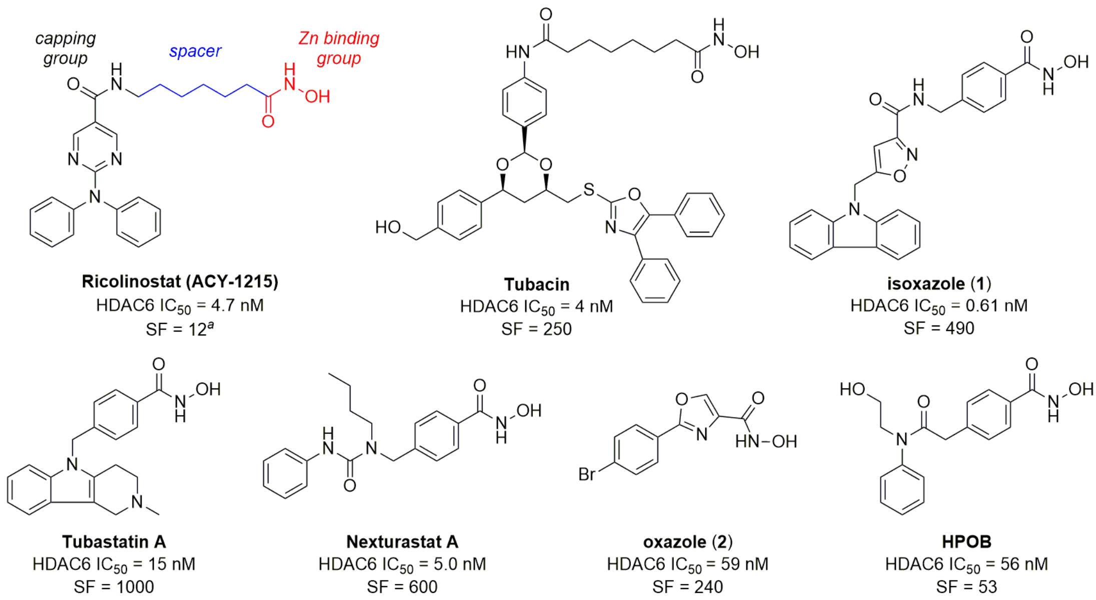

Figure 1. Selected examples of HDAC6 inhibitors: Ricolinostat (ACY-1215),[23] Tubacin,[24] isoxazole (**1**),[25] Tubastatin A,[26] Nexturastat A,[27] oxazole (**2**)[28] and HPOB.[29] Ricolinostat, tubacin and isoxazole (**1**) have been highlighted to show the typical HDACi pharmacophore of capping group-spacer-Zn binding group. [a] SF; selectivity for HDAC6 vs HDAC1.

Inhibitors of HDAC, regardless of whether they are pan-inhibitors or isoform specific, typically consist of a *zinc binding group* (ZBG) linked through a *spacer* to a *capping group* (highlighted as *red*, *blue* and *black* respectively in Figure 1).[31] The similarity between the active sites of the different isoforms makes achieving selectivity a non-trivial task and HDACi designed using the typical template are in many instances active against a number of isoforms.[32-34] Nevertheless, selectivity for HDAC6 has been successfully achieved through modifications of the capping group of the HDACi (see Figure 1) as this section of the inhibitor interacts with a region known to be less conserved amongst the HDAC family and hence is a valuable option for discrimination.[13, 26, 32] Similarly, it has been noted that the entrance to the active site of HDAC6 is slightly larger than that of the other isoforms and as a consequence HDAC6 selective inhibitors often feature a larger capping group (for example Tubacin and Tubastatin A, Figure 1).[24, 26, 35] The introduction of H-bond donor/acceptor groups to the capping group has also been shown to be an effective strategy for targeting HDAC6.[25, 29, 36, 37] Many of these HDAC6 selective inhibitors have been investigated as anticancer agents in their own right,[38] and considerable evidence is now available to support their use in combination therapy with other anticancer agents.[23, 39-42]

Many HDACi have therapeutic potential beyond cancer, for example, the well-known scriptaid (Figure 2) identified in 2000 by Su *et al*,[43, 44] has been investigated for the treatment of HIV, neurodegenerative disorders and to enhance muscle metabolism.[5, 45-47] Scriptaid is a hydroxamic acid-based inhibitor and its structure follows that of the archetypal HDAC pharmacophore.[13] Scriptaid has a modest preference for HDAC6,[‡ 48-50] yet, despite its well established anticancer activity,[51, 52] SAR studies regarding the capping group are limited, but do include a 3-nitro derivative[53] and a naphthalenediimide.[54] Other examples include 4-bromo, 4-alkyl and 3-hydroxy substituents on the naphthalimide ring, but these analogues employ the aminobenzamide moiety in place of the hydroxamic acid as the zinc-binding unit,[55] a modification known to favour class 1 HDAC inhibition.[56]

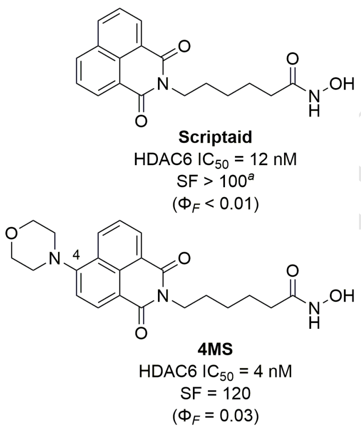

Figure 2. Structure of scriptaid and 4MS (Φ_F reported for DMSO).[50] [a] SF; selectivity for HDAC6 vs HDAC1.

In a recent report, a morpholine substituted scriptaid derivative (**4MS**, Figure 2) was identified as a fluorescent analogue that closely matched scriptaid in terms of inhibitory profile and *in vitro* activity.[50] A subsequent report by Zhang described a successful modification of **4MS** in which an arylhydroxamic acid (similar to tubastatin A) was used as the zinc binding unit.[57] Fluorescent molecular probes are of remarkable utility in elucidating and quantifying fundamental biological processes.[58-64] In addition, biologically active fluorescent compounds have great potential as theranostic agents.[65-69] Examples such as **4MS** are particularly valuable as, in contrast to the 'tagging' approach, only minor structural modifications are required to generate the fluorescent analogue and essential parameters such as molecular weight and polar surface area are not greatly impacted.

Although **4MS** is only weakly fluorescent (Φ_F = 0.03 in DMSO) rapid cellular uptake and subsequent localisation in the cytoplasm of human breast cancer (MDA-MB-231) cells was readily visualised.[50] Cytoplasmic localisation of HDACi has in itself been proposed as a means to elicit selectivity as HDAC6 is primarily found outside the nucleus.[66] Reports of fluorescent HDACi are not yet widespread in the literature,[57, 66, 70, 71] however, they have already been employed as displacement indicators[72] and theranostics.[66] Nevertheless, inhibitors that combine HDAC6 selectivity with strong fluorescence are rare.

1.1 Design

With the dual aims of (i) creating analogues with increased fluorescence quantum yields and (ii) investigating modifications to the capping group to enhance HDAC6 selectivity, we designed 4-amino analogues **3**–**8** for synthesis and evaluation in the current study (Figure 2, 4-aminoaryl **3** and **4**, 4-aminoalkyl **5**–**7**, and 4-nitro **8**). The aminobenzamide analogue of **4MS** was also of interest (**9**, Figure 2) for comparison against the aminobenzamide previously prepared by Delorme (**10**) that possessed no morpholine substituent at the 4-position of the naphthalimide ring.[55]

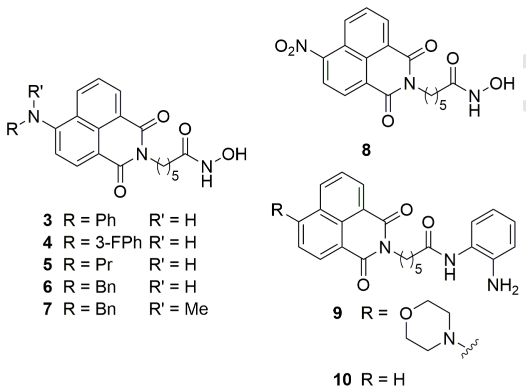

Figure 3. Design of scriptaid analogues **3–10** investigated herein.

The synthesis, together with the photophysical and biological evaluation, of this collection is presented herein. The utility of these compounds is demonstrated by cellular imaging and whole organism *in vivo* imaging, in which the distribution and the developmental impact of the inhibitors can be clearly visualised.

2 RESULTS AND DISCUSSION

2.1 Synthesis

In the 4-aminoscriptaid series, compound **7**, despite being disubstituted, was readily constructed; both the methylbenzyl and *N*-alkyl carboxylic acid moieties could be introduced in one-pot (Scheme 2).[73] Commercially available 4-chloronaphthalic anhydride **11** was heated with 6-aminohexanoic acid **13** and *N*-methylbenzylamine **12** using microwave irradiation at 140 °C for 30 mins to afford carboxylic acid **14** (70%, see ESI for full details). Conversion of the carboxylic acid **14** to the corresponding hydroxamic acid **7** was achieved using a two-step protocol involving (i) carbodiimide mediated coupling of commercially available *O*-(tetrahydro-2*H*-pyran-2-yl)hydroxylamine (NH_2OTHP) to the carboxylic acid, followed by (ii) deprotection of the *O*-protected hydroxamic acid under mild conditions (*p*-TsOH in *i*-PrOH).

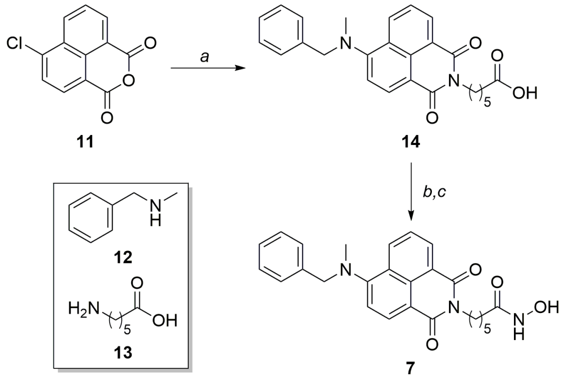

Scheme 1. Reagents and conditions: (a) **12**, **13**, DMSO, μw, 140 °C, 30 min; (b) NH_2OTHP, EDCI·HCl, HOBt, MeCN, 21 °C, 24 h (35%); (c) *p*-TsOH·H_2O, *i*-PrOH, 21 °C, 24 h (42%).

For the remainder of the 4-amino substituted analogues **3–6** the first step in the synthesis was the reaction of commercially available 4-bromo-1,8-naphthalic anhydride with methyl 6-aminohexanoate hydrochloride to give the corresponding imide **15** (Scheme 1). Heating imide **15** with the requisite amine in the presence of $Pd_2(dba)_3$·$CHCl_3$ (4 mol%), xantphos (4 mol%) and Cs_2CO_3 (3 equiv.) at 40 or 80 °C for 24 h afforded the desired aminonaphthalimides **16a–e** in high yields (81–98%).[74, 75] Hydrolysis gave the corresponding carboxylic acids **17a–d**, also in excellent yields (92–98%), and the hydroxamic acid was again installed using EDCI mediated coupling of NH_2OTHP and subsequent deprotection to give analogues **3**–**6**.

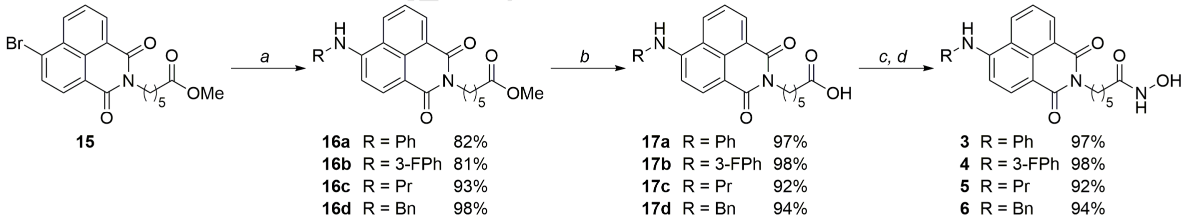

Scheme 2. Reagents and conditions: (a) $Pd_2(dba)_3$·$CHCl_3$ (4 mol%), xantphos (4 mol%), amine, Cs_2CO_3, $PhCH_3$, 40 or 80 °C, 24 h; (b) LiOH·H_2O, 1:1 THF/H_2O, 21 °C, 24 h; (c) NH_2OTHP, EDCI·HCl, HOBt, MeCN, 21 °C; (d) *p*-TsOH·H_2O, *i*-PrOH, 21 °C.

The 4-nitro derivative **8** was synthesised in a similar fashion using a three-step sequence starting with commercially available 4-nitronaphthalic anhydride **18** (Scheme 3).

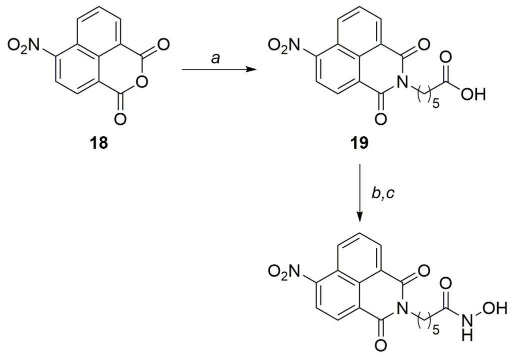

Scheme 3: Reagents and conditions: (a) **13**, EtOH, MW, 100 °C, 60 min (76%); (b) NH_2OTHP, EDCI·HCl, HOBt, MeCN, 21 °C, 24 h (50%); (c) *p*-TsOH·H_2O, *i*-PrOH, 80 °C, 16 h (33%).

The aminobenzamide analogues of **4MS** and scriptaid were accessed from the carboxylic acid precursors **20**[50] and **21**, the latter prepared from naphthalic anhydride (See ESI for full details). Treatment of the acids with 1,2-diaminobenzene, EDCI·HCl and HOBt[55] gave the target compounds, **9** and **10** in yields of 67% and 43%, respectively (Scheme 4).

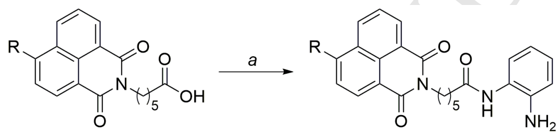

Scheme 4. Reagents and conditions: (a) *o*-phenylenediamine, EDCI·HCl, HOBt, MeCN, 21 °C, 24 h.

2.2 HDAC Isoform Inhibition.

The scriptaid analogues were assessed for inhibitory activity against HDAC isoforms 1, 3 and 8 (class I), HDAC6 (class IIb) and HDAC11 (class IV). Hydroxamic acids bearing nitrogen containing substituents in the 4-position (**3**–**7**) typically inhibited HDAC6 at least as effectively as scriptaid (IC_{50} = 12 nM). Of these examples, the propylamine and benzylamine substituted derivatives **5** and **6** possessed low nanomolar activity (IC_{50} = 4.8 and 3.5 nM respectively); better than scriptaid and comparable to that of HDAC6 selective HDACi rocilinostat[23] and nexturastat[27] (HDAC6 IC_{50} of 4.7 and 5.0 nM respectively). The 4-anilino **3** and **4** mirrored scriptaid in terms of potency towards HDAC6 (IC_{50} = 13 and 14 nM respectively).

It is noteworthy that the *N*-alkyl compounds (**5**–**7**) showed significantly enhanced selectivity for HDAC6 over HDAC1 (Table 1), which compares well against scriptaid and known HDAC6 specific agents. The most potent of these (**5** and **6**) were subsequently evaluated against the remaining HDAC isoforms (HDAC2, 4, 5, 7 9 and 10, see ESI S2.1) and compound **6** was identified as more than 500-fold selective for HDAC6 compared with HDAC1 (IC_{50} = 1.98 μM), 100-fold more selective against HDAC3 (IC_{50} = 0.36 μM) and 190-fold more selective against the other class IIb isoform HDAC10

(IC_{50} = 0.66 µM). The enhanced selectivity of compound **6** for HDAC6 over HDAC1 exceeds that of the reported HPOB[29] and HPB[37] and also Tubacin[24] and Tubastatin A.[26]

The presence of the aminobenzamide ZBG typically favours inhibition at class I HDACs, and this preference was observed for **9** and **10**, with no activity at both HDAC6 and HDAC8 below the starting concentration (10 µM) of the assay. Both of these derivatives exhibited sub-micromolar inhibition of HDAC3 (IC_{50} = 0.29 and 0.20 µM for **9** and **10**, respectively) and HDAC1 (IC_{50} = 0.43 and 0.74 µM) with reasonable selectivity against HDAC11.

Table 1: Inhibition of individual HDAC isoforms, IC_{50} (µM)[a] and the selectivity factor[b] (SF) vs HDAC6.

Compound	**HDAC Isoform (SF)**[b]				
	1	**3**	**6**	**8**	**11**
TSA	0.032 ± 0.009 (5)	0.013 ± 0.003 (2)	0.0059 ± 0.001	0.99 ± 0.11 (167)	0.015 ± 0.006 (2)
scriptaid	1.74 ± 0.04 (145)	0.37 ± 0.04 (31)	0.012 ± 0.002	1.52 ± 0.007 (127)	0.36 ± 0.02 (30)
4MS	1.43 ± 0.09 (119)	0.32 ± 0.03 (27)	0.012 ± 0.001	1.81 ± 0.12 (151)	0.29 ± 0.01 (24)
3	2.38 ± 0.007 (183)	0.47 ± 0.003 (36)	0.013 ± 0.0006	4.09 ± 0.02 (315)	0.19 ± 0.01 (14)
4	3.06 ± 0.16 (219)	0.55 ± 0.01 (39)	0.014 ± 0.002	4.07 ± 0.05 (291)	0.21 ± 0.001 (15)
5	0.59 ± 0.02 (123)	0.11 ± 0.004 (23)	0.0048 ± 0.0002	1.52 ± 0.08 (317)	0.08 ± 0.03 (16)
6	1.98 ± 0.04 (566)	0.36 ± 0.0007 (103)	0.0035 ± 0.0002	2.46 ± 0.11 (703)	0.15 ± 0.02 (43)
7	2.38 ± 0.06 (245)	0.70 ± 0.003 (72)	0.0097 ± 0.0007	1.40 ± 0.03 (144)	1.22 ± 0.13 (126)
8	0.63 ± 0.09 (111)	1.62 ± 0.06 (284)	0.0057 ± 0.0007	0.62 ± 0.02 (109)	1.02 ± 0.11 (179)
9	0.43 ± 0.03 (-)[c]	0.29 ± 0.01 (-)	>10 (-)	>10 (-)	8.12 ± 0.91 (-)
10	0.74 ± 0.06 (-)	0.20 ± 0.004 (-)	>10 (-)	>10 (-)	9.35 ± 0.96 (-)

[a] IC_{50} performed in duplicate using 10-dose IC_{50} mode with 3-fold serial dilution starting from 10 µM solutions; [b] Selectivity for HDAC6 over other isoforms calculated by dividing the IC_{50} value for the relevant isoform against that for HDAC6. [c] Not determined due to lack of HDAC6 activity.

Given that the naphthalimide core, the linker and ZBG are identical for scriptaid, **4MS** and compounds **3**–**8** the strong and selective inhibition of HDAC6 observed for compounds **5**–**7** could reasonably be attributed to additional interactions of the position 4 substituents of the naphthalimide with the residues surrounding the rim of the active site; a region less conserved across the various HDAC isoforms.[13, 26, 32]

2.3 Molecular Modelling

To shed more light on the observed results a number of compounds (scriptaid, **4MS** and compounds **3–8**) were docked into the active site of HDAC6 (co-crystallised with TSA; PDB accession code:

5EDU).[76] As expected the *N*-alkyl hydroxamic acid projects away from the heterocyclic core through the tunnel towards the zinc ion of the active site. This perpendicular geometry is common for 1,8-naphthlaimides as it relieves steric strain between the carbonyl groups of the imide substituent.[77] In each case the 1,8-napthalimide core sits close to the solvent exposed surface of the enzyme and is largely solvent exposed itself. The proximity of this ring system to the protein surface appears to be governed by the minimised conformation of the 4-substituent, which is in turn accommodated by flexibility in the linker portion of the molecule.

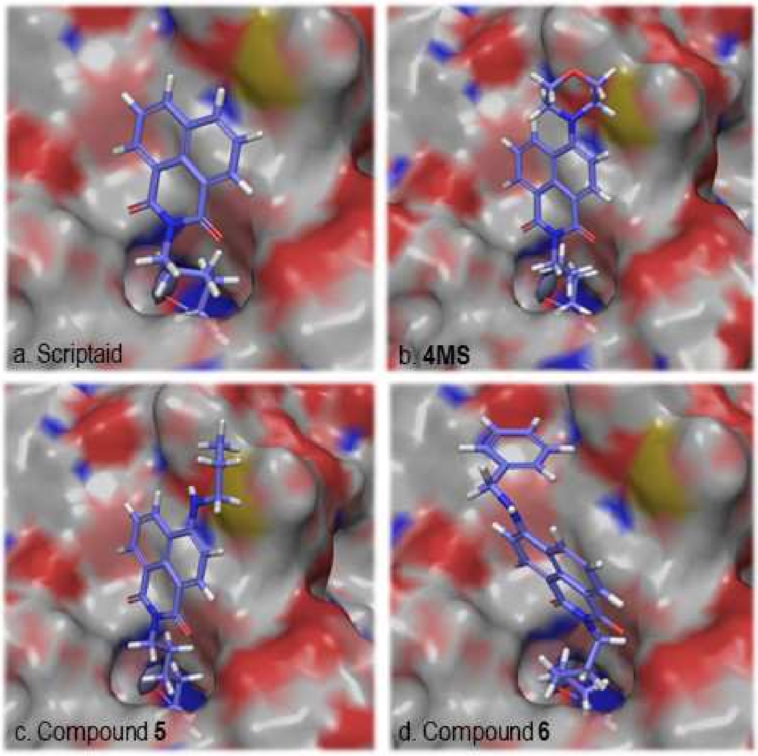

Figure 4: Docking of (a) Scriptaid, (b) **4MS** and compounds (c) **5** and (d) **6** with the crystal structure of HDAC6 obtained by removing bound trichostatin.[76] The potential for additional hydrophobic interactions of the N-substituent of **5** (b) and **6** (c) with the surface of HDAC6 can be clearly seen.

For **4MS** and **3** the inhibition at HDAC6 is equivalent to that of scriptaid (0.012, 0.013 and 0.012 µM respectively). These results are in accordance with the absence of any additional interactions (e.g. electrostatic). For compounds **5** and **6** which displayed ~2-fold better inhibition (4.8 and 3.7 nM, respectively) it could be rationalised that the heterocyclic ring could adopt two possible conformations which are "flipped" with relation to each other (Figure 4b and c). Additional flexibility of the aliphatic substituent may serve to increase van der Waals interactions with the protein surface. Whereas analogue **3** (4-NHPh) does not have the flexibility to adopt such a pose (Figure S3.1).

2.4 Activity against KASUMI-1 cancer cells

Cancer is an established target for many HDACi including scriptaid[51, 52] and as such the *in-vitro* antiproliferative activity of the new scriptaid analogues to inhibit cell growth was evaluated in KASUMI-1 cell lines (Table 2, see ESI section S4 for details). Compared to scriptaid, slightly enhanced activity was noted for compounds **3**–**6**. The 4-propylamino derivative **5** was of interest, inhibiting the growth of the KASUMI-1 cell line with an IC_{50} of 0.096 µM, a five-fold improvement over scriptaid (0.49 µM, Table 2). Of interest, the aminobenzamide analogues targeting HDAC1 (**9** and **10**) were less effective than scriptaid in this assay. Given HDAC1 is primarily localised in the nucleus the lesser activity is potentially a result of poor nuclear penetration.

Table 2. Anticancer activity in the KASUMI-1 cell line.[a]

Compound	IC_{50} (µM)
scriptaid	0.49[b]
4MS	0.29
3	0.28
4	0.32
5	0.096
6	0.36
7	0.81
8	0.57
9	0.64
10	1.09

[a] Compounds were incubated with KASUMI-1 cells for 72 hr then viability determined using resazurin reagent. IC_{50} values were determined from the mean of three experiments conducted in duplicate. [b] Error < 1% (n = 3). See ESI section S4 for full details.

2.5 Photophysical Evaluation

The absorption and emission spectra obtained for compounds **3**–**7** (Table 3) are typical for 4-aminonaphthalimides with $\lambda_{abs} \approx 440$ nm, $\lambda_{em} \approx 530$ nm in DMSO and $\lambda_{abs} \approx 440$ nm, $\lambda_{em} \approx 540$ nm in aqueous buffer.[78, 79] Of particular relevance to the aim of developing potent and highly fluorescent scriptaid analogues, several of the most biologically active compounds were also strongly fluorescent, for example, the quantum yield for propyl analogue **5** ($\Phi_F = 0.81$ in DMSO and $\Phi_F = 0.28$ in buffer) made this compound ideally suited for further studies. In contrast, the 4-*N*-phenyl analogues (**3** and **4**) were weakly fluorescent ($\Phi_F < 0.01$), as was the disubstituted 4-NBn(Me)N **7** ($\Phi_F = 0.07$ in DMSO). For **3** and **4** the electron withdrawing aryl group restricts electron transfer to the ICT system and for disubstituted **7** the steric clash between the 4-amino-substituents and the hydrogen at the 5-position (*peri* position) disfavours the planar structure required for ICT.[80]

Table 3. Photophysical properties of selected compounds in DMSO and aqueous buffer.

Compound	Solvent[a]	λ_{abs} (nm)[b]	λ_{em} (nm)[b]	Stokes Shift	Φ_F[c]
scriptaid	DMSO	336	386	50	<0.01
	PB	-	-	-	-
4MS[50]	DMSO	399	534	135	0.03
	PB	396	460	64	<0.01
3	DMSO	448	544	99	<0.01
	PB	-	-	-	-
4	DMSO	443	536	93	<0.01
	PB	-	-	-	-
5	DMSO	446	526	80	0.81
	PB	456	548	92	0.28
6	DMSO	439	523	84	0.83
	PB	446	543	97	0.38
7	DMSO	422	528	106	0.07
	PB	431	544	113	0.15
9	DMSO	402	535	133	0.04
	PB	-	-	-	-

[a] PB = 1% DMSO in 10 mM phosphate buffer (pH 7.40); [b] Wavelengths of maximum absorbance (λ_{abs}) and emission intensity (λ_{em}); [c] Values represent the average of three measurements.

2.6 Cellular Imaging

To examine cellular uptake and localisation, A549 cells were incubated with the most promising candidates **5**, and **6** (1 μM) for 20 mins and 2 hours (Figure 5). As a representative of the aminobenzamide class of inhibitors compound **9** was also included in the cellular imaging studies.

Cellular fluorescence was visualised by confocal microscopy following excitation with a 405 nm laser. All three dyes showed good intracellular fluorescence, with clear localisation in the cytoplasm and similar intracellular fluorescence intensities for all three compounds. Localisation did not change markedly over time. There was a distinct lack of fluorescence within nuclear regions and we have previously shown that **4MS** fluorescence is not quenched in the presence of DNA,[50] indicating that the lack of fluorescence in the nucleus is due to a lack of nuclear accumulation rather than due to quenching of fluorescence by DNA

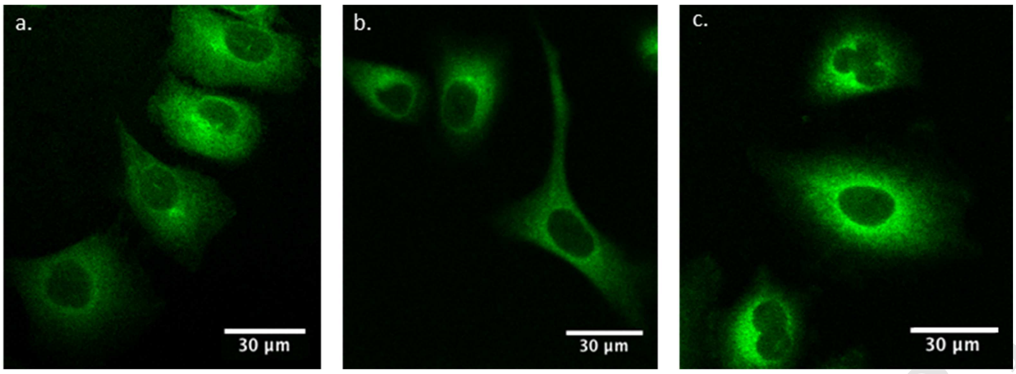

Figure 5: Confocal microscopy images of A549 cells incubated for 2 hours with (a) **5**, (b) **6**, (c) **9**, (1 µM, λ_{ex} = 405 nm, λ_{em} = 460–560 nm) highlighting uptake and cytoplasmic distribution.

The aminobenzamide **9** showed some degree of lysosomal, as well as cytoplasmic, localisation. (Figure 6). An established method of lysosomal targeting uses tertiary amines such as the morpholine group, which can be protonated in the acidic environment of the lysosome, preventing diffusion back into the cytoplasm.[81] However, for compound **9**, the morpholine nitrogen is conjugated with the aromatic naphthalimide system, reducing basicity and explaining why only partial accumulation in the lysosomes was observed. This partial localisation was confirmed with co-localisation studies with Lysotracker Red, with a Pearson's correlation coefficient of 0.58 (Figure S6.3). The localisation study supports the postulation above that the inability of the compound to access HDAC1 in the nucleus leads to decreased activity. For compound **6** at 10 µM incubation, protrusions of the membrane were observed (Figure 6). Such blebbing is the initial phase of cell disassembly in apoptosis, consistent with the cytotoxicity of these compounds.

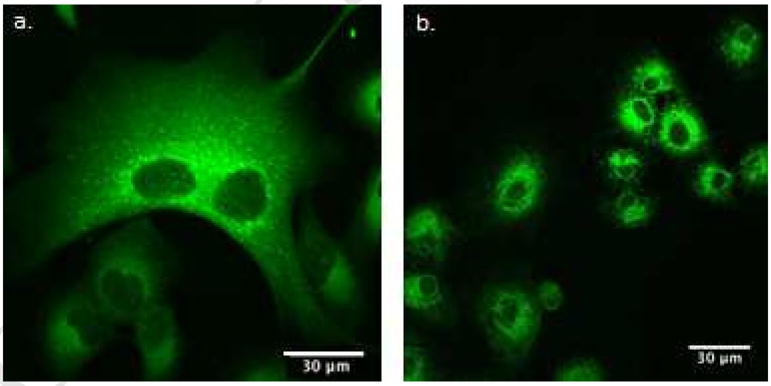

Figure 6: Confocal microscopy image (λ_{ex} = 405 nm, λ_{em} = 460–560 nm) of A549 cells incubated with (a) **9** at 1 µM for 2 hours with punctate staining consistent with lysosomal localisation and (b) **6** at 10 µM for 20 minutes showing blebbing consistent with toxicity.

2.7 Zebrafish imaging

Of the analogues prepared, the 4-aminopropyl and the benzyl analogues **5** and **6** exhibited favourable properties in terms of HDAC6 activity, selectivity, cellular potency and high fluorescence quantum yields, and were therefore selected for further *in vivo* studies using developing zebrafish embryos.

Class IIa HDACs are known to be distributed in the heart, brain and skeletal muscle (for HDAC4, 5, 9) and in the heart, skeletal muscle, pancreas and placenta for HDAC7, while Class IIb HDAC have been detected in the heart, liver, kidney, placenta and vascular system (HDAC6) and in the liver spleen and kidney (HDAC10).[20]

In order to characterise whole organism localisation a time course study was performed in which zebrafish embryos were treated with 1, 10 and 20 µM of **5** or **6** from 24–50 hours post fertilization (hpf) for 24 hours. Following the incubation of the fluorescent scriptaid derivatives, imaging experiments were performed 72 hpf, (Figure 7, See ESI section S7 for fluorescent images for analogue **5** and superimposed fluorescence & brightfield images for **5** and **6**). Due to strong autofluorescence from the yolk sac (correlating with the known high lipid content), fluorescence from derivatives **5** and **6** was only clearly visualised posterior to the yolk sac extension, specifically in the trunk and tail. Again autofluorescence was noted in this section (due to melanocytes in the dorsal section), however, for the zebrafish treated at 10 and 20 µM the distribution of the fluorescent analogues **5** and **6** could be clearly visualised—confirming ready uptake of the compounds and localisation in the vasculature; a site rich in HDAC6. Compounds **5** and **6** have high affinity for HDAC6 *in-vitro*, however, it is impossible to state unequivocally that this determines their *in vivo* behaviour as distribution is influenced by a number of factors.[82] A similar scenario, involving the distribution of fluorescent naphthalimide based Zn binders in zebrafish, was encountered by Goldup and Watkinson.[83, 84]

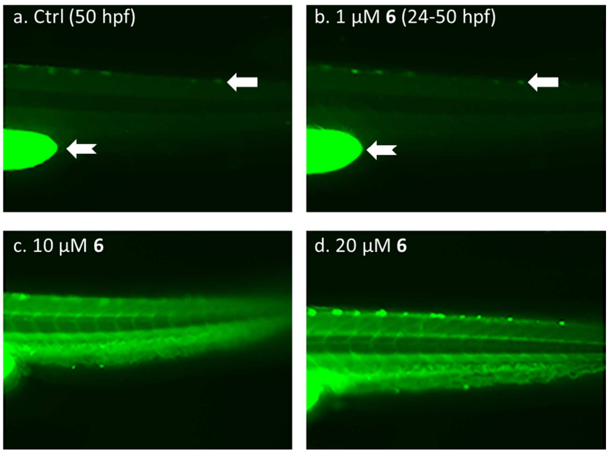

Figure 7: Fluorescent images of posterior trunk and tail section of zebrafish embryo after exposure to **6**. Zebrafish were exposed to (a) 0, (b) 1, (c) 10 or (d) 20 µM of **6** during the time period 24–50 hpf and visualised 72 hpf using fluorescence microscopy (λ_{ex} = 480 nm, λ_{em} = 517 nm). Arrows highlight auto-fluorescence due to lipids in the yolk sac and also from melanocytes in the dorsal section.

The pan-inhibitor Trichostatin A (TSA) has been shown to have a strong effect on blood vessel formation in developing zebrafish embryos.[85] An additional HDAC6 specific transient knock-down study in zebrafish has clearly demonstrated that the absence of this isoform results in malformations of the vascular system, including vessel maturation, an outcome that matches those identified in a mouse model.[17] To investigate the impact of **5** and **6** on organism development, zebrafish embryos were exposed from 24–50 hours post fertilisation (hpf) to 10 μM of **5** and **6** with scriptaid and Trichostatin A (TSA) employed as controls. The vascular system was visualised at 72 hours by alkaline phosphatase staining (Figure 8).[86]

All compounds had a negative impact on blood vessel development especially the formation of the subintestinal vein, the blood vessel that lies on the top of the yolk sac. These results confirm that, like the known HDAC inhibitors, analogues **5** and **6** affect blood vessel formation. However, compared to the damage resulting from exposure to TSA and even scriptaid, the subintestinal vein defects caused by compounds **5** and **6** were not as pronounced. Given that the new analogues would be expected to have similar pharmacokinetic behaviour to scriptaid, and at 10 μM they are clearly present in the vasculature (indicated by the fluorescence studies outlined above), it is postulated that the improved selectivity of both **5** and **6** for HDAC6 leads to the milder phenotype that was observed, corroborating the idea that selectively targeting HDAC6 leads to 'viable' organisms.[20, 21, 86]

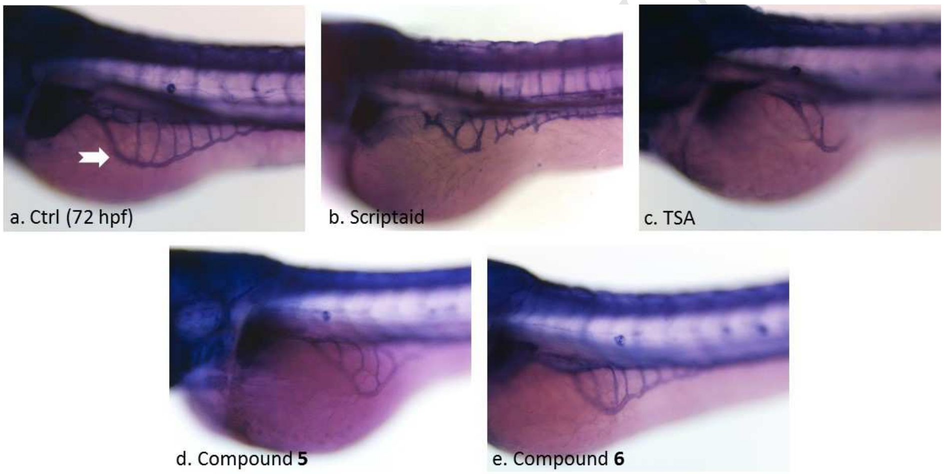

Figure 8. Images of Zebrafish embryos 72 hpf after treatment with HDACi. All compounds were used at a concentration of 10 μM. Embryos were exposed from 24-50 hpf with (a) vehicle only, (b) scriptaid (10 μM), (c) TSA (10 μM), (d) **5** (10 μM) and (e) **6** (10 μM) and stained at 72 hpf with alkaline phosphatase to visualise blood vessels.

3 CONCLUSION

This study has identified a number of scriptaid analogues that inhibit HDAC6 as effectively as known inhibitors rocilinostat and nexturastat and are also highly selective (compound **6** is more than 500 fold selective for HDAC6 over HDAC1). Furthermore, the compounds are highly fluorescent and both their distribution and activity confirmed in a zebrafish model organism. It is expected that these compounds will be of considerable use to researchers examining the biological effects of scriptaid and the selective inhibition of HDAC6.

4 EXPERIMENTAL SECTION

General reagents and solvents for the synthesis of compounds were purchased from commercial sources and used as supplied. Column chromatography was performed using 230–400 Mesh silica gel. Melting points are uncorrected. All NMR spectra (^{1}H and ^{13}C) were collected on a 270, 400 or 500 MHz spectrometer as specified. Samples were dissolved (0.5 mL) in either deuterated chloroform ($CDCl_3$) or deuterated dimethyl sulfoxide (DMSO-*d*$_6$). NMR chemical shifts were assigned using 2D NMR experiments (HSQC and HMBC). In instances when either the ^{1}H or ^{13}C resonance was coincidental with the deuterated solvent or residual H_2O, the resonance was confirmed by HSQC experiments. High Resolution Mass Spectra (HRMS) analysis were conducted and recorded on an HRMS-ESI-TOF. Those reactions that employed microwave irradiation were conducted using a CEM Discover S-Class Microwave reactor, operating at a frequency of 50/60 Hz and continuous irradiation power from 0 to 200 W. Reaction mixture temperatures were monitored by an external infrared sensor. All reactions were conducted in either 10 mL or 35 mL microwave vials sealed with a Teflon® crimp cap.

6-(6-(Benzyl(methyl)amino)-1,3-dioxo-1*H*-benzo[*de*]isoquinolin-2(3*H*)-yl)hexanoic acid (14)

In a 5 mL microwave vial, a mixture of 4-chloro-1,8-naphthalic anhydride **11** (235 mg, 1.01 mmol), 6-aminohexanoic acid **13** (131 mg, 0.999 mmol) and *N*-benzylmethylamine **12** (390 µL, 3.02 mmol) in DMSO (2 mL) was heated using microwave irradiation at 140 °C for 30 min. The reaction mixture was diluted with H_2O (15 mL) and acidified with 2 M HCl (5 mL) and extracted using EtOAc (2 × 30 mL). The combined organic phase was washed with brine (30 mL), dried ($MgSO_4$), filtered and concentrated under reduced pressure. The crude solid was then triturated in 2 M HCl (20 mL) to afforded the title compound **14** (305 mg, 70%), as an orange solid, which was then used in the following step without further purification; ^{1}H NMR (500 MHz, DMSO-*d*$_6$): δ 11.98 (s, 1H, COOH), 8.52 (d, *J* = 8.5 Hz, 1H, H-9), 8.45 (d, *J* = 7.6 Hz, 1H, H-7), 8.34 (d, *J* = 8.1 Hz, 1H, H-4), 7.75 (dd, *J* = 8.4, 7.3 Hz, 1H, H-8), 7.40–7.33 (m, 4H, Ar, H-5), 7.32–7.27 (m, 2H, Ar), 4.58 (s, 2H, CH_2Ar), 4.01 (t, *J* = 7.5 Hz, H-6'), 2.95 (s, 3H, NCH_3), 2.21 (t, *J* = 7.3 Hz, 2H, H-2'), 1.64–1.58 (m, 2H, H-3'/H-5'), 1.57–1.51 (m, 2H, H-3'/H-5'), 1.37–1.29 (m, 2H, H-4'); ^{13}C NMR (125 MHz, DMSO-*d*$_6$): δ 174.5, 163.6, 163.0, 155.8, 137.3, 132.1, 130.7 (C × 2), 129.5, 128.6 (C × 2), 127.7 (C × 2), 127.4, 126.0, 125.0, 122.5, 115.0, 114.4, 60.1, 41.5, 39.7, 33.5, 27.4, 26.1, 24.2; HRMS (*m/z*, ESI$^+$): Calculated for $C_{26}H_{26}N_2O_4$ *m/z* = 413.1971 [M+H]$^+$. Found *m/z* = 431.1978.

6-(6-(Benzyl(methyl)amino)-1,3-dioxo-1*H*-benzo[*de*]isoquinolin-2(3*H*)-yl)-*N*-hydroxyhexanamide (7)

A mixture of 6-(6-(benzyl(methyl)amino)-1,3-dioxo-1*H*-benzo[*de*]isoquinolin-2(3*H*)-yl)hexanoic acid **14** (110 mg, 0.256 mmol), EDCI·HCl (83 mg, 0.433 mmol), anhydrous HOBt (17 mg, 0.126 mmol) and *O*-(tetrahydro-2*H*-pyran-2-yl)hydroxylamine (62 mg, 0.529 mmol) in MeCN (5 mL) was stirred at 21 °C for 24 h. The precipitate that had formed in solution was collected by vacuum filtration to afford the THP-protected hydroxamic acid (47 mg, 35%) as a yellow solid; ^{1}H NMR (270 MHz, DMSO-d_6): δ 10.88 (s, 1H), 8.54 (d, J = 8.4 Hz, 1H), 8.47 (d, J = 7.2 Hz, 1H), 8.35 (d, J = 7.9 Hz, 1H), 7.77 (app. t, $J_{app.}$ = 7.9 Hz, 1H), 7.46–7.24 (m, 6H), 4.74 (s, 1H), 4.59 (s, 2H), 4.01 (t, J = 7.3 Hz, 2H), 3.92–3.83 (m, 1H), 3.45–3.37 (m, 1H), 2.96 (s, 3H), 1.98 (t, J = 7.1 Hz, 2H), 1.71–1.38 (m, 10H), 1.35–1.27 (m, 2H); ^{13}C NMR (125 MHz, DMSO-d_6): δ 169.0, 163.6, 163.0, 155.8, 137.3, 132.1, 130.7 (C × 2), 129.5, 128.6 (C × 2), 128.0 (C × 2), 127.4, 125.6, 125.0, 122.6, 115.0, 114.4, 100.8, 61.2, 60.0, 41.5, 39.5, 32.1, 27.8, 27.4, 26.0, 24.7, 24.6, 18.3. Next, a solution of the THP-protected hydroxamic acid (28 mg, 0.053 mmol) in 2-propanol (1 mL) was treated with TsOH·H_2O (1 mg, 0.005 mmol) at 50 °C for 16 h. During this time a yellow precipitate formed in solution which was isolated by vacuum filtration to afford the title compound **7** (10 mg, 42%) as a bright yellow solid; ^{1}H NMR (500 MHz, DMSO-d_6): δ 10.31 (s, 1H, N*H*OH), 8.65 (s, 1H, NHO*H*), 8.54 (d, J = 8.5 Hz, 1H, H-9), 8.47 (d, J = 6.6 Hz, 1H, H-7), 8.36 (d, J = 8.2 Hz, 1H, H-4), 7.77 (app. t, $J_{app.}$ = 7.5 Hz, 1H, H-8), 7.42–7.33 (m, 4H, Ar), 7.32–7.28 (m, 2H, H-5, Ar), 4.59 (s, 2H, CH_2Ar), 4.01 (t, J = 7.4 Hz, 2H, H-6'), 2.96 (s, 3H, CH_3), 1.95 (t, J = 7.3 Hz, 2H, H-2'), 1.64–1.58 (m, 2H, H-3'/H-5'), 1.57–1.48 (m, 2H, H-3'/H-5'), 1.33–1.27 (m, 2H, H-4'); ^{13}C NMR (125 MHz, DMSO-d_6): δ 169.0, 163.6, 163.0, 155.8, 137.3, 132.1, 130.70, 130.67, 129.5, 128.6 (C × 2), 127.7 (C × 2), 127.4, 125.6, 125.0, 122.6, 115.0, 114.4, 60.0, 41.5, 39.8, 32.1, 27.4, 26.1, 24.9; m.p. 136–138 °C; HRMS (*m/z*, ESI$^+$): Calculated for $C_{26}H_{28}N_3O_4$ *m/z* = 446.2074 [M+H]$^+$. Found *m/z* = 446.2076.

6-(1,3-Dioxo-6-(phenylamino)-1*H*-benzo[*de*]isoquinolin-2(3*H*)-yl)hexanoic acid (17a)

A solution of methyl 6-(1,3-dioxo-6-(phenylamino)-1*H*-benzo[*de*]isoquinolin-2(3H)-yl)hexanoate **16a** (160 mg, 0.38 mmol) and LiOH·H_2O (161 mg, 3.84 mmol) in THF/H_2O (1:1, 3 mL) was stirred at 21 °C for 24 h. The solvent volume was halved *in vacuo* and the remaining mixture was diluted with H_2O and treated with 2 M HCl until pH 3 was obtained. The resulting precipitate was collected by vacuum filtration to afford the title compound **17a** (148 mg, 97%) as a yellow solid; ^{1}H NMR (270 MHz, DMSO-d_6): δ 9.40 (s, 1H, NH), 8.82 (d, J = 8.5 Hz, 1H, H-9), 8.50 (d, J = 7.2 Hz, 1H, H-7), 8.27 (d, J = 8.5 Hz, 1H, H-4), 7.79 (app. t, $J_{app.}$ = 8.3 Hz, 1H, H-8), 7.49–7.38 (m, 4H, H-2'', H-3'', H-5'', H-6''), 7.26–7.16 (m, 2H, H-5, H-4''), 4.01 (t, J = 7.2 Hz, 2H, H-6'), 2.21 (t, J = 7.2 Hz, 2H, H-2'), 1.67–1.49 (m, 4H, H-3', H-5'), 1.38–1.27 (m, 2H, H-4'); ^{13}C NMR (125 MHz, DMSO-d_6): δ 174.5, 163.7, 162.8, 147.9, 140.4, 133.5, 131.1, 129.6 (C × 2), 129.5, 129.0, 125.1, 124.2, 122.7 (C × 2), 122.1, 121.6, 111.1, 107.8, 39.0, 33.7, 27.4, 26.1, 24.3; m.p. 119–122 °C; HRMS (*m/z*, ESI$^+$): Calculated for $C_{24}H_{23}N_2O_4$ *m/z* = 403.1652[M+H]$^+$. Found *m/z* = 403.1659.

6-(6-((3-Fluorophenyl)amino)-1,3-dioxo-1*H*-benzo[*de*]isoquinolin-2(3*H*)-yl)hexanoic acid (17b)

A solution of methyl 6-(6-((3-fluorophenyl)amino)-1,3-dioxo-1*H*-benzo[*de*]isoquinolin-2(3*H*)-yl)hexanoate **16b** (174 mg, 0.40 mmol) and LiOH·H_2O (167 mg, 4.00 mmol) in THF/H_2O (1:1, 3 mL) was stirred at 21 °C for 24 h. The solvent volume was halved *in vacuo* and the remaining mixture was diluted with H_2O and treated with 2 M HCl until pH 3 was obtained. The resulting precipitate was collected by vacuum filtration to afford the title compound **17b** (164 mg, 98%) as an orange solid; ^{1}H NMR (500 MHz, DMSO-d_6): δ 11.98 (br s, 1H, COOH), 9.42 (s, 1H, NH), 8.73 (dd, J = 8.5, 0.8 Hz, 1H, H-9), 8.47 (dd, J = 7.4, 0.8 Hz, 1H, H-7), 8.29 (d, J = 8.4 Hz, 1H, H-4), 7.79 (dd, J = 8.5, 7.4 Hz, 1H, H-8), 7.46–7.42 (m, 1H, H-5''), 7.40 (d, J = 8.4 Hz, 1H, H-5), 7.22 (d, J = 8.1, Hz, 1H, H-6''), 7.18 (dt, J = 11.0, 2.1 Hz, 1H, H-2''), 6.94 (td, J = 8.4, 2.1 Hz, 1H, H-4''), 3.99 (t, J = 7.5 Hz, 2H, H-6'), 2.21 (t, J = 7.4 Hz, 2H, H-2'), 1.64–1.58 (m, 2H, H-5'), 1.57–1.51 (m, 2H, H-3'), 1.36–1.30 (m, 2H, H-4'); ^{13}C NMR (125 MHz, DMSO-d_6): δ 174.4, 163.6, 162.80 (d, $^1J_{C-F}$ = 241.5 Hz), 162.78, 146.6, 142.8 (d, $^3J_{C-F}$ = 10.0 Hz), 133.1, 131.06 (d, $^3J_{C-F}$ = 8.8 Hz), 131.05, 129.3, 129.0, 125.4, 122.2, 122.1, 117.3 (d, $^4J_{C-F}$ = 1.3 Hz), 112.3, 109.9 (d, $^2J_{C-F}$ = 21.3 Hz), 109.3, 108.1 (d, $^2J_{C-F}$ = 23.8 Hz), 39.6, 33.5, 27.3, 26.1, 24.2; m.p. 88–90 °C; HRMS (*m/z*, ESI$^+$): Calculated for $C_{24}H_{22}FN_2O_4$ *m/z* = 421.1558 [M+H]$^+$. Found *m/z* = 421.1558.

6-(1,3-Dioxo-6-(propylamino)-1*H*-benzo[*de*]isoquinolin-2(3*H*)-yl)hexanoic acid (17c)

A solution of methyl 6-(1,3-dioxo-(6-propylamino)-1*H*-benzo[*de*]isoquinolin-2(3*H*)-yl)hexanoate **16c** (54 mg, 0.14 mmol) and LiOH·H_2O (60 mg, 1.44 mmol) in THF/H_2O (1:1, 2 mL) was stirred at 21 °C for 24 h. The solvent volume was halved *in vacuo* and the remaining mixture was diluted with H_2O and treated with 2 M HCl until pH 3 was obtained. The resulting precipitate was collected by vacuum filtration to afford the title compound **17c** (47 mg, 92%) as an orange solid; ^{1}H NMR (270 MHz, DMSO-d_6): δ 11.98 (br s, 1H, COOH), 8.72 (dd, J = 8.6, 1.2 Hz, 1H, H-9), 8.43 (dd, J = 7.3, 1.0 Hz, 1H, H-7), 8.26 (d, J = 8.7 Hz, 1H, H-4), 7.80 (t, J = 5.6 Hz, 1H, NH), 7.68 (dd, J = 8.4, 7.3 Hz, 1H, H-8), 6.78 (d, J = 8.7 Hz, 1H, H-5), 3.99 (t, J = 7.4 Hz, 2H, H-6'), 3.35 (2H, $CH_2CH_2CH_3$)^α, 2.21 (t, J = 7.3 Hz, 2H, H-2'), 1.80–1.66 (m, 2H, $CH_2CH_2CH_3$), 1.65–1.43 (m, 4H, H-3', H-5'), 1.39–1.26 (m, 2H, H-4'), 0.99 (t, J = 7.4 Hz, 3H, $CH_2CH_2CH_3$); ^{13}C NMR (125 MHz, DMSO-d_6): δ 174.4, 163.8, 162.9, 150.7, 134.3, 130.7, 129.5, 128.6, 124.2, 121.9, 120.1, 107.5, 103.8, 44.6, 39.2, 33.5, 27.4, 26.1, 24.2, 21.2, 11.6; m.p. 211–213 °C; HRMS (*m/z*, ESI$^+$): Calculated for $C_{21}H_{25}N_2O_4$ *m/z* = 369.1809 [M+H]$^+$. Found *m/z* = 369.1823. ^{α} *Confirmed by HSQC.*

6-(6-(Benzylamino)-1,3-dioxo-6-1*H*-benzo[*de*]isoquinolin-2(3*H*)-yl)hexanoic acid (17d)

A solution of methyl 6-(6-(benzylamino)-1,3-dioxo-1*H*-benzo[*de*]isoquinolin-2(3*H*)-yl)hexanoate **16d** (55 mg, 0.13 mmol) and LiOH·H_2O (54 mg, 1.28 mmol) in THF/H_2O (1:1, 2 mL) was stirred at 21 °C for 24 h. The solvent volume was halved *in vacuo* and the remaining mixture was diluted with H_2O and treated with 2 M HCl until pH 3 was obtained. The resulting precipitate was collected by vacuum filtration to afford the title compound **17d** (50 mg, 94%) as a bright yellow solid; ^{1}H NMR (270 MHz, DMSO-d_6): δ 8.78 (d, J = 8.7 Hz, 1H, H-9), 8.50 (t, J = 6.1 Hz, 1H, NH), 8.45 (d, J = 7.5 Hz, 1H, H-7), 8.17 (d, J = 8.6 Hz, 1H, H-4), 7.73 (app. t, $J_{app.}$ = 7.4 Hz, 1H, H-8), 7.42–7.22 (m, 5H, Ar), 6.67 (d, J = 8.6 Hz, 1H, H-5), 4.67 (d, J = 6.1 Hz, 2H, CH_2Ar), 3.98 (t, J = 7.4 Hz, 2H, H-6'), 2.20 (t, J = 7.4 Hz, 2H, H-2'), 1.64–1.47 (m, 4H, H-3', H-5'), 1.36–1.23 (m, 2H, H-4'); ^{13}C NMR (125 MHz, DMSO-d_6): δ 174.5, 163.7, 162.9, 150.4, 138.5, 134.0, 130.8, 129.4, 128.6 (C × 3), 127.1, 127.0 (C × 2), 124.6, 122.0, 120.3, 108.1, 104.6, 45.9, 39.1, 33.5, 27.4, 26.1, 24.3; m.p. 191–192 °C; HRMS (*m/z*, ESI$^+$): Calculated for $C_{25}H_{25}N_2O_4$ *m/z* = 417.1809 [M+H]$^+$. Found *m/z* = 417.1829.

6-(1,3-Dioxo-6-(phenylamino)-1*H*-benzo[*de*]isoquinolin-2(3*H*)-yl-*N*-hydroxyhexanamide (3)

A mixture of 6-(1,3-dioxo-6-(phenylamino)-1*H*-benzo[*de*]isoquinolin-2(3*H*)-yl)hexanoic acid **17a** (156 mg, 0.388 mmol), EDCI·HCl (90 mg, 0.582 mmol), anhydrous HOBt (26 mg, 0.194 mmol) and *O*-(tetrahydro-2*H*-pyran-2-yl)hydroxylamine (95 mg, 0.815 mmol) in MeCN (8 mL) was stirred at 21 °C for 24 h. After solvent was removed, the crude material was then suspended in H_2O (10 mL) and extracted with EtOAc (3 × 30 mL). The combined organic phase was washed with KH_2PO_4 (10 mL) and brine (10 mL), dried ($MgSO_4$), filtered and concentrated under reduced pressure. Purification by flash column chromatography (9:1 CH_2Cl_2/MeOH with 1% NH_4OH) afforded the THP-protected hydroxamic acid (144 mg, 74%, R_f = 0.50) as an orange solid; ^{1}H NMR (500 MHz, DMSO-d_6): δ 10.89 (s, 1H), 9.41 (s, 1H), 8.83 (d, J = 8.4 Hz, 1H), 8.50 (d, J = 7.2 Hz, 1H), 8.27 (d, J = 8.5 Hz, 1H), 7.80 (app. t, $J_{app.}$ = 7.9 Hz, 1H), 7.46 (app. t, $J_{app.}$ = 7.7 Hz, 2H), 7.40 (d, J = 7.8 Hz, 2H), 7.25 (d, J = 8.5 Hz, 1H), 7.19 (t, J = 7.3 Hz, 1H), 4.76–4.72 (m, 1H), 4.01 (t, J = 7.4 Hz, 2H), 3.92–3.84 (m, 1H), 3.45–3.39 (m, 1H), 1.98 (t, J = 7.3 Hz, 2H), 1.65–1.38 (m, 10H), 1.35–1.25 (m, 2H); ^{13}C NMR (125 MHz, DMSO-d_6): δ 169.0, 163.7, 162.9, 147.9, 140.4, 133.5, 131.1, 129.6 (C × 2), 129.5, 129.0, 125.2, 124.2, 122.7 (C × 2), 122.1, 121.6, 111.1, 107.8, 100.8, 61.3, 39.8, 32.0, 27.8, 27.4, 26.0, 24.8, 24.7, 18.3. Next, a solution of THP-protected hydroxamic acid (78 mg, 0.156 mmol) in 2-propanol (3 mL) was treated with TsOH·H_2O (9 mg, 0.047 mmol). The reaction mixture was allowed to stir at 40 °C for 16 h, during which, a red precipitate formed in solution. The precipitate was isolated by vacuum filtration to afford the title compound **3** (39 mg, 60%) as a red solid; ^{1}H NMR (270 MHz, DMSO-d_6): δ 10.35 (br s, 1H, N*H*OH), 9.40 (s, 1H, NHO*H*), 8.83 (d, J = 8.4 Hz, 1H, H-9), 8.65 (s, 1H, NH), 8.50 (d, J = 7.4 Hz, 1H, H-7), 8.28 (d, J = 8.5 Hz, 1H, H-4), 7.80 (app. t, $J_{app.}$ = 7.6 Hz, 1H, H-8), 7.49–7.38 (m, 4H, H-2'', H-3'', H-5'', H-6''), 7.25 (d, J = 8.5 Hz, 1H, H-5), 7.19 (t, J = 7.1 Hz, 1H, H-4''), 4.01 (t, J = 7.1 Hz, 2H, H-6'), 1.95 (t, J = 7.1 Hz, 2H, H-2'), 1.66–1.48 (m, 4H, H-3', H-5'), 1.35–1.23 (m, 2H, H-4'); ^{13}C NMR (125 MHz, DMSO-d_6): δ 169.5, 164.1, 163.3, 148.4, 140.8, 133.9, 131.5, 130.02 (C × 2), 130.00, 129.6, 125.6, 124.7, 123.2 (C × 2), 122.5, 122.1, 111.5, 108.2, 39.5, 32.6, 27.9, 26.6, 25.4; m.p. 188–190 °C; HRMS (*m/z*, ESI$^+$): Calculated for $C_{24}H_{24}N_3O_4$ *m/z* = 418.1761 [M+H]$^+$. Found *m/z* = 418.1774.

6-(6-((3-Fluorophenyl)amino)-1,3-dioxo-1*H*-benzo[*de*]isoquinolin-2(3*H*)-yl)-*N*-hydroxyhexanamide (4)

A mixture of 6-(6-((3-fluorophenyl)amino)-1,3-dioxo-1*H*-benzo[*de*]isoquinolin-2(3*H*)-yl)hexanoic acid **17b** (167 mg, 0.397 mmol), EDCI·HCl (92 mg, 0.596 mmol), anhydrous HOBt (27 mg, 0.199 mmol) and *O*-(tetrahydro-2*H*-pyran-2-yl)hydroxylamine (98 mg, 0.834 mmol) in MeCN (9 mL) was stirred at 21 °C for 48 h. The reaction mixture was cooled (0 °C) and the precipitate isolated by vacuum filtration to afford the THP-protected hydroxamic acid (120 mg, 58%) as a bright yellow solid; ^{1}H NMR (270 MHz, DMSO-d_6): δ 10.89 (s, 1H), 9.46 (s, 1H), 8.77 (dd, J = 8.5, 1.0 Hz, 1H), 8.51 (dd, J = 7.3, 1.0 Hz, 1H), 8.32 (d, J = 8.4 Hz, 1H), 7.83 (dd, J = 8.5, 7.4 Hz, 1H), 7.53–7.35 (m, 2H), 7.29–7.10 (m, 3H), 7.03–6.84 (m, 1H), 4.74 (s, 1H), 4.02 (t, J = 7.2 Hz, 2H), 3.94–3.75 (m, 1H), 3.51–3.37 (m, 1H), 1.99 (t, J = 7.3 Hz, 2H), 1.70–1.39 (m, 10H), 1.38–1.22 (m, 2H); ^{13}C NMR (125 MHz, DMSO-d_6): δ 169.0, 163.6, 162.9, 162.8 (d, $^1J_{C\text{-}F}$ = 241.5 Hz), 146.6, 142.9 (d, $^3J_{C\text{-}F}$ = 10.6 Hz), 133.2, 131.13, 131.11 (d, $^3J_{C\text{-}F}$ = 9.5 Hz), 129.4, 129.1, 125.5, 122.3, 122.2, 117.3, 112.4, 110.2 (d, $^2J_{C\text{-}F}$ = 29.9 Hz), 109.4, 108.1 (d, $^2J_{C\text{-}F}$ = 23.7 Hz), 100.8, 61.2, 39.7, 32.0, 27.8, 27.4, 26.0, 24.8, 24.7, 18.3. Next, a solution of THP-protected hydroxamic acid (63 mg, 0.121 mmol) in 2-propanol (4 mL) was treated with TsOH·H_2O (7 mg, 0.036 mmol). The reaction mixture was allowed to stir at 40 °C for 16 h, during which, an orange precipitate formed in solution. The precipitate was isolated by vacuum filtration to afford the title compound **4** (40 mg, 77%) as an orange solid; ^{1}H NMR (270 MHz, DMSO-d_6): δ 10.33 (s, 1H, N*H*OH), 9.46 (s, 1H, NHO*H*), 8.77 (d, J = 8.5 Hz, 1H, H-9), 8.66 (br s, 1H, NH), 8.51 (d, J = 7.1 Hz, 1H, H-7), 8.33 (d, J = 8.4 Hz, 1H, H-4), 7.83 (app. t, $J_{app.}$ = 7.9 Hz, 1H, H-8), 7.50–7.41 (m, 2H, H-5, H-5''), 7.24–7.17 (m, 2H, H-2'', H-6''), 6.95 (td, J = 8.7, 2.3 Hz, 1H, H-4''), 4.01 (t, J = 7.2 Hz, 2H, H-6'), 1.95 (t, J = 7.2 Hz, 2H, H-2'), 1.69–1.46 (m, 4H, H-3', H-5'), 1.35–1.26 (m, 2H, H-4'); ^{13}C NMR (125 MHz, DMSO-d_6): δ 169.5, 164.1, 163.28 (d, $^1J_{C\text{-}F}$ = 241.3 Hz), 163.26, 147.1, 143.3 (d, $^3J_{C\text{-}F}$ = 10.4 Hz), 133.7, 131.5 (d, $^3J_{C\text{-}F}$ = 9.8 Hz), 129.8, 129.6, 129.4, 125.9, 122.7, 122.6, 117.7 (d, $^4J_{C\text{-}F}$ = 1.9 Hz), 112.8, 110.4 (d, $^2J_{C\text{-}F}$ = 20.9 Hz), 109.8, 108.6 (d, $^2J_{C\text{-}F}$ = 23.9 Hz), 39.5, 32.6, 27.9, 26.6, 25.4; m.p. 193–195 °C; HRMS (*m/z*, ESI$^+$): Calculated for $C_{24}H_{23}FN_3O_4$ *m/z* = 436.1667 [M+H]$^+$. Found *m/z* = 436.1665.

6-(1,3-Dioxo-6-(propylamino)-1*H*-benzo[*de*]isoquinolin-2(3*H*)-yl)-*N*-hydroxyhexanamide (5)

A mixture containing 6-(1,3-dioxo-6-(propylamino)-1*H*-benzo[*de*]isoquinolin-2(3*H*)-yl)hexanoic acid **17c** (244 mg, 0.662 mmol), EDCI·HCl (226 mg, 1.46 mmol), anhydrous HOBt (45 mg, 0.331 mmol) and *O*-(tetrahydro-2*H*-pyran-2-yl)hydroxylamine (163 mg, 1.39 mmol) in CH_2Cl_2 (20 mL) was stirred at 21 °C for 48 h. The reaction mixture was then transferred into a separatory funnel and washed with KH_2PO_4 (10 mL) and brine (10 mL), dried ($MgSO_4$), filtered and concentrated under reduced pressure. Purification by flash column chromatography (9:1 CH_2Cl_2/MeOH with 1% NH_4OH) afforded the THP-protected hydroxamic acid (262 mg, 85%, R_f = 0.58) as a yellow solid; ^{1}H NMR

(500 MHz, DMSO-d_6): δ 10.88 (s, 1H), 8.71 (dd, *J* = 8.6, 1.2 Hz, 1H), 8.42 (dd, *J* = 7.3, 1.0 Hz, 1H), 8.25 (d, *J* = 8.5 Hz, 1H), 7.79 (t, *J* = 5.5 Hz, 1H), 7.67 (dd, *J* = 8.5, 7.3 Hz, 1H), 6.78 (d, *J* = 8.7 Hz, 1H), 4.76–4.73 (m, 1H), 3.99 (t, *J* = 7.4 Hz, 2H), 3.90–3.83 (m, 1H), 3.47–3.40 (m, 1H), 3.34 (2H)$^{\alpha}$, 1.98 (t, *J* = 7.3 Hz, 2H), 1.74–1.68 (m, 2H), 1.62–1.43 (m, 10H), 1.28–1.25 (m, 2H), 0.99 (t, *J* = 7.4 Hz); ^{13}C NMR (125 MHz, DMSO-d_6): δ 169.0, 163.8, 162.9, 150.7, 134.3, 130.7, 129.5, 128.6, 124.2, 121.9, 120.1, 107.5, 103.8, 100.8, 61.3, 44.6, 39.3, 32.1, 28.8, 27.5, 26.0, 24.7, 21.2, 19.6, 18.3, 11.6. Next, a solution of THP-protected hydroxamic acid (239 mg, 0.511 mmol) in 2-propanol (3 mL) was added TsOH·H_2O (30 mg, 0.153 mmol). The reaction mixture was allowed to stir at 21 °C for 16 h, during which, a fine yellow precipitate formed in solution. The solvent was removed under reduced pressure and crude material was triturated in MeCN (1 mL) at 21 °C for 12 h to afford the title compound **5** (52 mg, 27%) as yellow solid; ^{1}H NMR (400 MHz, DMSO-d_6): δ 10.32 (s, 1H, N*H*OH), 8.72 (d, *J* = 8.8 Hz, 1H, H-9), 8.65 (s, 1H, NHO*H*), 8.44 (d, *J* = 7.3 Hz, 1H, H-7), 8.27 (d, *J* = 8.8 Hz, 1H, H-4), 7.79 (t, *J* = 5.4 Hz, 1H, NH), 7.68 (app. t, $J_{app.}$ = 8.3 Hz, 1H, H-8), 6.79 (d, *J* = 8.8 Hz, 1H, H-5), 3.99 (t, *J* = 7.3 Hz, 2H, H-6'), 3.37 (2H, $CH_2CH_2CH_3$)$^{\alpha}$, 1.95 (t, *J* = 7.4 Hz, 2H, H-2'), 1.77–1.68 (m, 2H, $CH_2CH_2CH_3$), 1.62–1.49 (m, 4H, H-3', H-5'), 1.32–1.23 (m, 2H, H-4'), 0.99 (t, *J* = 7.3 Hz, 3H, $CH_2CH_2CH_3$); ^{13}C NMR (125 MHz, DMSO-d_6): δ 169.5, 164.2, 163.4, 151.2, 134.8, 131.1, 129.9, 129.0, 124.7, 122.3, 120.5, 107.9, 104.3, 45.0, 39.6, 32.6, 28.0, 26.6, 25.4, 21.6, 12.0; m.p. 194–196 °C; HRMS (*m/z*, ESI$^+$): Calculated for $C_{21}H_{26}N_3O_4$ *m/z* = 384.1918 [M+H]$^+$. Found *m/z* = 384.1933. $^{\alpha}$ *Confirmed by HSQC.*

6-(6-(Benzylamino)-1,3-dioxo-6-1*H*-benzo[*de*]isoquinolin-2(3*H*)-yl)-*N*-hydroxyhexanamide (6)

A mixture of 6-(6-benzylamino)-1,3-dioxo-1*H*-benzo[*de*]isoquinolin-2(3*H*)-yl)hexanoic acid **17d** (338 mg, 0.812 mmol), EDCI·HCl (277 mg, 1.79 mmol), anhydrous HOBt (55 mg, 0.406 mmol) and *O*-(tetrahydro-2*H*-pyran-2-yl)hydroxylamine (200 mg, 1.71 mmol) in CH_2Cl_2 (20 mL) was stirred at 21 °C for 48 h. The reaction mixture was then transferred into a separatory funnel and washed with KH_2PO_4 (10 mL) and brine (10 mL), dried ($MgSO_4$), filtered and concentrated under reduced pressure. Purification by flash column chromatography (9:1 CH_2Cl_2/MeOH with 1% NH_4OH) afforded the THP-protected hydroxamic acid (358 mg, 86%, R_f = 0.55) as a yellow solid; ^{1}H NMR (500 MHz, DMSO-d_6): δ 10.88 (s, 1H), 8.77 (dd, *J* = 8.5, 1.1 Hz, 1H), 8.49 (t, *J* = 6.1 Hz, 1H), 8.45 (dd, *J* = 7.4, 1.0 Hz, 1H), 8.16 (d, *J* = 8.6 Hz, 1H), 7.73 (dd, *J* = 8.4, 7.3 Hz, 1H), 7.40 (d, *J* = 6.9 Hz, 2H), 7.33 (t app., $J_{app.}$ = 7.6 Hz, 2H), 7.24 (t, *J* = 7.3 Hz, 1H), 6.67 (d, *J* = 8.6 Hz, 1H), 4.75–4.72 (m, 1H), 4.66 (d, *J* = 5.9 Hz, 2H), 3.97 (t, *J* = 7.4 Hz, 2H), 3.89–3.82 (m, 1H), 3.44–3.38 (m, 1H), 1.97 (t, *J* = 7.3 Hz, 2H), 1.60–1.41 (m, 10H), 1.30–1.22 (m, 2H); ^{13}C NMR (125 MHz, DMSO-d_6): δ 169.0, 163.7, 162.9, 150.4, 138.5, 134.0, 130.7, 129.4, 128.5 (C × 3), 127.02, 126.92 (C × 2), 124.6, 122.0, 120.3, 108.2, 104.6, 100.8, 61.3, 45.9, 39.5, 32.0, 27.8, 27.5, 26.0, 24.8, 24.7, 18.3. Next, a solution of THP-protected hydroxamic acid (93 mg, 0.180 mmol) in 2-propanol (2 mL) was treated with TsOH·H_2O (10 mg, 0.054 mmol). The reaction mixture was allowed to stir at 21 °C for 16 h, during which, a fine yellow precipitate formed in solution. The solvent was removed under reduced pressure and the crude material was triturated in MeCN (1 mL) at 21 °C for 12 h to afford the title compound **6** (43 mg, 56%) as yellow solid; ^{1}H NMR (500 MHz, DMSO-d_6): δ 10.31 (s, 1H, N*H*OH), 8.78 (d, *J* = 8.4 Hz, 1H, H-9), 8.65 (s, 1H, NHO*H*), 8.50 (t, *J* = 6.0 Hz, 1H, NH), 8.46 (d, *J* = 7.2 Hz, 1H, H-7), 8.17 (d, *J* = 8.5 Hz, 1H, H-4), 7.73 (app. t, $J_{app.}$ = 7.9 Hz, 1H, H-8), 7.40 (d, *J* = 7.6 Hz, 2H, H-2'', H-6''), 7.34 (app. t, $J_{app.}$ = 7.6 Hz, 2H, H-3'', H-5''), 7.25 (app. t, $J_{app.}$ = 7.3 Hz, 1H, H-4''), 6.68 (d, *J* = 8.6 Hz, 1H, H-5), 4.67 (d, *J* = 5.9 Hz, 2H, CH_2Ar), 3.97 (t, *J* = 7.5 Hz, 2H, H-6'), 1.93 (t, *J* = 7.3 Hz, 2H, H-2'), 1.61–1.47 (m, 4H, H-3', H-5'), 1.31–1.23 (m, 2H, H-4'); ^{13}C NMR (125 MHz, DMSO-d_6): δ 169.1, 163.8, 162.9, 150.4, 138.5, 134.1, 130.8, 129.4, 128.6 (C × 3), 127.1, 127.0 (C × 2), 124.6, 122.0, 120.3, 108.1, 104.6, 45.9, 39.1, 32.2, 27.5, 26.2, 25.0; m.p. 179–182 °C; HRMS (*m/z*, ESI$^+$): Calculated for $C_{25}H_{26}N_3O_4$ *m/z* = 432.1917 [M+H]$^+$. Found *m/z* = 432.1930.

N-Hydroxy-6-(6-nitro-1,3-dioxo-1*H*-benzo[*de*]isoquinolin-2(3*H*)-yl)hexanamide (8)

A mixture of 6-(6-nitro-1,3-dioxo-1*H*-benzo[*de*]isoquinolin-2(3*H*)-yl)hexanoic acid **19** (315 mg, 0.884 mmol), EDCI·HCl (206 mg, 1.33 mmol), anhydrous HOBt (60 mg, 0.442 mmol) and *O*-(tetrahydro-2*H*-pyran-2-yl)hydroxylamine (217 mg, 1.86 mmol) in MeCN (20 mL) was stirred at 21 °C for 24 h. The solvent was removed under reduced pressure and the resulting crude residue was triturated in MeCN (2 mL) to afford the THP-protected hydroxamic acid (247 mg, 50%) as a tan solid; ^{1}H NMR (270 MHz, DMSO-d_6): δ 10.88 (s, 1H), 8.71 (dd, *J* = 8.7, 1.0 Hz, 1H), 8.63 (dd, *J* = 7.3, 1.1 Hz, 1H), 8.61 (d, *J* = 8.1 Hz, 1H), 8.55 (d, *J* = 8.1 Hz, 1H), 8.10 (dd, *J* = 8.7, 7.3 Hz, 1H), 4.71 (s, 1H), 4.03 (t, *J* = 7.3 Hz, 2H), 3.93–3.76 (m, 1H), 3.41–3.37 (m, 1H), 1.98 (t, *J* = 7.3 Hz, 2H), 1.70–1.38 (m, 10H), 1.38–1.26 (m, 2H); ^{13}C NMR (125 MHz, DMSO-d_6): δ 168.9, 163.0, 162.2, 149.2, 131.7, 130.1, 129.6, 128.8, 128.4, 126.7, 124.3, 122.83, 122.78, 100.7, 61.2, 39.6, 32.0, 27.7, 27.2, 25.9, 24.7, 24.6, 18.2. Next, a solution of the THP-protected hydroxamic acid (112 mg, 0.246 mmol) in 2-propanol (3 mL) was added TsOH·H_2O (13 mg, 0.074 mmol). The reaction mixture was allowed to stir at 80 °C for 16 h, during which, a tan precipitate formed in solution. The precipitate was isolated by vacuum filtration and triturated in MeCN (1 mL) to afford the title compound **8** (30 mg, 33%) as a tan solid; ^{1}H NMR (270 MHz, DMSO-d_6): δ 10.33 (s, 1H, N*H*OH), 8.72 (d, *J* = 8.7 Hz, 1H, H-9), 8.68–8.59 (m, 2H, H-4, H-7), 8.56 (d, *J* = 8.0 Hz, 1H, H-5), 8.10 (dd, *J* = 8.7, 7.4 Hz, 1H, H-8), 4.03 (t, *J* = 7.4 Hz, 2H, H-6'), 1.95 (t, *J* = 7.3 Hz, 2H, H-2'), 1.74–1.45 (m, 4H, H-3', H-5'), 1.42–1.23 (m, 2H, H-4'); ^{13}C NMR (125 MHz, DMSO-d_6): δ 169.1, 163.0, 162.2, 149.2, 131.8, 130.2, 129.7, 129.0, 128.8, 128.5, 126.7, 124.3, 122.8, 39.6, 32.1, 27.2, 26.1, 24.9; m.p. 175–177 °C; HRMS (*m/z*, ESI$^+$): Calculated for $C_{18}H_{17}N_3O_6$ *m/z* = 372.1196 [M+H]$^+$. Found *m/z* = 372.1201.

N-(2-Aminophenyl)-6-(6-morpholino-1,3-dioxo-1*H*-benzo[*de*]isoquinolin-2(3*H*)-yl)hexanamide (9)

To a mixture of 6-(6-morpholino-1,3-dioxo-1*H*-benzo[*de*]isoquinolin-2(3*H*)-yl)hexanoic acid **20** (266 mg, 0.671 mmol) in MeCN (15 mL), was added EDCI·HCl (229 mg, 1.48 mmol), anhydrous HOBt (45 mg, 0.336 mmol) and *O*-phenylenediamine (152 mg, 1.48 mmol). After stirring at 21 °C for 24 h, the solvent was removed under reduced pressure. Purification by flash column chromatography (9:1 CH_2Cl_2/MeOH with 1% NH_4OH) afforded the title compound **9** (219 mg, 67%, R_f = 0.50) as a yellow solid; ^{1}H NMR (500 MHz, DMSO-d_6): δ 9.06 (s, 1H, NH), 8.51–8.49 (m, 2H, H-7, H-9), 8.43 (d, J = 8.1 Hz, 1H, H-4), 7.82 (dd, J = 8.5, 7.4 Hz, 1H, H-8), 7.37 (d, J = 8.2 Hz, 1H, H-5), 7.10 (dd, J = 7.8, 1.2 Hz, H-6'''), 6.87 (td, J, = 7.3, 1.4 Hz, 1H, H-4'''), 6.69 (dd, J = 8.0, 1.3 Hz, H-3'''), 6.49 (td, J, = 7.7, 1.4 Hz, 1H, H-5'''), 4.79 (s, 2H, NH_2), 4.05 (t, J = 7.4 Hz, 2H, H-6'), 3.91 (app. t, $J_{app.}$ = 4.7 Hz, 4H, H-2'', H-6''), 3.23 (app. t, $J_{app.}$ = 4.5 Hz, 4H, H-3'', H-5''), 2.31 (t, J = 7.4 Hz, 2H, H-2'), 1.69–1.61 (m, 4H, H-3', H-5'), 1.41–1.35 (m, 2H, H-4'); ^{13}C NMR (125 MHz, DMSO-d_6): δ 171.1, 163.6, 163.1, 155.5, 141.9, 132.2, 130.7, 130.6, 129.2, 126.2, 125.7, 125.32, 125.29, 123.5, 122.6, 116.1, 115.9, 115.8, 115.2, 66.2 (C × 2), 53.1 (C × 2), 39.8, 35.6, 27.5, 26.2, 25.1; m.p. 66–67 °C; HRMS (*m/z*, ESI$^+$): Calculated for $C_{28}H_{31}N_4O_4$ *m/z* = 487.2340 $[M+H]^+$. Found *m/z* = 487.2341.

5 ASSOCIATED CONTENT

Supporting Information. Full ^{1}H NMR and ^{13}C NMR spectra of novel compounds. This material is available free of charge via the Internet at…….

6 AUTHOR INFORMATION

Corresponding Author

*Phone: +613 5227 1439. Email: fred.pfeffer@deakin.edu.au

Author Contributions

All authors contributed equally and have given approval of the final version of the manuscript.

Funding Sources

Notes

The authors declare no competing financial interests.

7 ACKNOWLEDGEMENT

CLF and TDA thank the Centre for Chemistry and Biotechnology at Deakin University for a top up scholarship and a salary contribution respectively. The work performed by YG was supported by grants from the Centre for Molecular and Medicinal research at Deakin University. YG and PY thank the Deakin University zebrafish facility. We thank Westpac Bicentennial Foundation for a Research Fellowship (EJN) and the Australian government for a Research Training Program Scholarship (KGL). The authors acknowledge Alexander P. Ray for helping with the *in vivo* experiments in zebrafish and the scientific and technical assistance of the Australian Microscopy and Microanalysis Research Facility at the Australian Centre for Microscopy and Microanalysis (ACMM) at the University of Sydney.

8 ABBREVIATIONS

HDAC: histone deacetylase

HDACi: histone deacetylase inhibitor

hpf: hours post fertilisation

9 FOOTNOTES

‡ The degree of HDAC6 selectivity (vs HDAC1) reported for scriptaid varies from simply suggested (Langley *et al*.),[48] to 6-fold (Yanik *et al*. and Bradner *et al*.),[49, 87] to >100 (Fleming *et al*.).[50] There are reports (Cremer *et al*.) indicating scriptaid favours HDAC1 over HDAC6.[88]

10 REFERENCES

1. Johnstone, R. W., Histone-deacetylase inhibitors: novel drugs for the treatment of cancer. *Nature reviews Drug discovery* **2002,** *1* (4), 287-299.
2. Bolden, J. E.; Peart, M. J.; Johnstone, R. W., Anticancer activities of histone deacetylase inhibitors. *Nature reviews Drug discovery* **2006,** *5* (9), 769-784.
3. Witt, O.; Deubzer, H. E.; Milde, T.; Oehme, I., HDAC family: What are the cancer relevant targets? *Cancer Lett* **2009,** *277* (1), 8-21.
4. Kim, H.-J.; Bae, S.-C., Histone deacetylase inhibitors: molecular mechanisms of action and clinical trials as anti-cancer drugs. *American journal of translational research* **2011,** *3* (2), 166.
5. Falkenberg, K. J.; Johnstone, R. W., Histone deacetylases and their inhibitors in cancer, neurological diseases and immune disorders. *Nat Rev Drug Discov* **2014,** *13* (9), 673-91.
6. West, A. C.; Johnstone, R. W., New and emerging HDAC inhibitors for cancer treatment. *J Clin Invest* **2014,** *124* (1), 30-9.
7. Marks, P. A.; Breslow, R., Dimethyl sulfoxide to vorinostat: development of this histone deacetylase inhibitor as an anticancer drug. *Nature Biotechnology* **2007,** *25*, 84.
8. Prince, H. M.; Dickinson, M., Romidepsin for Cutaneous T-cell Lymphoma. *Clinical Cancer Research* **2012,** *18* (13), 3509-3515.
9. O'Connor, O. A.; Horwitz, S.; Masszi, T.; Hoof, A. V.; Brown, P.; Doorduijn, J.; Hess, G.; Jurczak, W.; Knoblauch, P.; Chawla, S.; Bhat, G.; Choi, M. R.; Walewski, J.; Savage, K.; Foss, F.; Allen, L. F.; Shustov, A., Belinostat in Patients With Relapsed or Refractory Peripheral T-Cell Lymphoma: Results of the Pivotal Phase II BELIEF (CLN-19) Study. *Journal of Clinical Oncology* **2015,** *33* (23), 2492-2499.

10. Raedler, L. A., Farydak (Panobinostat): First HDAC Inhibitor Approved for Patients with Relapsed Multiple Myeloma. *American Health & Drug Benefits* **2016,** *9* (Spec Feature), 84-87.
11. Shuai, G.; Xiaoyang, L.; Jie, Z.; Wenfang, X.; Yingjie, Z., Preclinical and Clinical Studies of Chidamide (CS055/HBI-8000), An Orally Available Subtype-selective HDAC Inhibitor for Cancer Therapy. *Anti-Cancer Agents in Medicinal Chemistry* **2017,** *17* (6), 802-812.
12. Daniel, A. R.; Sreekanth, T.; Carlos, A. M. F., Beyond the Selective Inhibition of Histone Deacetylase 6. *Mini-Reviews in Medicinal Chemistry* **2016,** *16* (14), 1175-1184.
13. Roche, J.; Bertrand, P., Inside HDACs with more selective HDAC inhibitors. *Eur J Med Chem* **2016,** *121*, 451-483.
14. Wang, X.-X.; Wan, R.-Z.; Liu, Z.-P., Recent advances in the discovery of potent and selective HDAC6 inhibitors. *European Journal of Medicinal Chemistry* **2018,** *143*, 1406-1418.
15. Miyake, Y.; Keusch, J. J.; Wang, L.; Saito, M.; Hess, D.; Wang, X.; Melancon, B. J.; Helquist, P.; Gut, H.; Matthias, P., Structural insights into HDAC6 tubulin deacetylation and its selective inhibition. *Nat Chem Biol* **2016,** *12* (9), 748-54.
16. Kalin, J. H.; Bergman, J. A., Development and Therapeutic Implications of Selective Histone Deacetylase 6 Inhibitors. *Journal of Medicinal Chemistry* **2013,** *56* (16), 6297-6313.
17. Kaluza, D.; Kroll, J.; Gesierich, S.; Yao, T. P.; Boon, R. A.; Hergenreider, E.; Tjwa, M.; Rossig, L.; Seto, E.; Augustin, H. G.; Zeiher, A. M.; Dimmeler, S.; Urbich, C., Class IIb HDAC6 regulates endothelial cell migration and angiogenesis by deacetylation of cortactin. *EMBO J* **2011,** *30* (20), 4142-56.
18. Hai, Y.; Christianson, D. W., Histone deacetylase 6 structure and molecular basis of catalysis and inhibition. *Nat. Chem. Biol.* **2016,** *12* (9), 741-7.
19. Li, Y.; Shin, D.; Kwon, S. H., Histone deacetylase 6 plays a role as a distinct regulator of diverse cellular processes. *FEBS Journal* **2013,** *280* (3), 775-793.
20. Haberland, M.; Montgomery, R. L.; Olson, E. N., The many roles of histone deacetylases in development and physiology: implications for disease and therapy. *Nature Reviews Genetics* **2009,** *10*, 32.
21. Dallavalle, S.; Pisano, C.; Zunino, F., Development and therapeutic impact of HDAC6-selective inhibitors. *Biochemical Pharmacology* **2012,** *84* (6), 756-765.
22. Tavares, M. T.; Shen, S.; Knox, T.; Hadley, M.; Kutil, Z.; Bařinka, C.; Villagra, A.; Kozikowski, A. P., Synthesis and Pharmacological Evaluation of Selective Histone Deacetylase 6 Inhibitors in Melanoma Models. *ACS Medicinal Chemistry Letters* **2017,** *8* (10), 1031-1036.
23. Santo, L.; Hideshima, T.; Kung, A. L.; Tseng, J.-C.; Tamang, D.; Yang, M.; Jarpe, M.; van Duzer, J. H.; Mazitschek, R.; Ogier, W. C.; Cirstea, D.; Rodig, S.; Eda, H.; Scullen, T.; Canavese, M.; Bradner, J.; Anderson, K. C.; Jones, S. S.; Raje, N., Preclinical activity, pharmacodynamic, and pharmacokinetic properties of a selective HDAC6 inhibitor, ACY-1215, in combination with bortezomib in multiple myeloma. *Blood* **2012,** *119* (11), 2579-2589.
24. Haggarty, S. J.; Koeller, K. M.; Wong, J. C.; Grozinger, C. M.; Schreiber, S. L., Domain-selective small-molecule inhibitor of histone deacetylase 6 (HDAC6)-mediated tubulin deacetylation. *Proceedings of the National Academy of Sciences* **2003,** *100* (8), 4389-4394.
25. Gaisina, I. N.; Tueckmantel, W.; Ugolkov, A.; Shen, S.; Hoffen, J.; Dubrovskyi, O.; Mazar, A.; Schoon, R. A.; Billadeau, D.; Kozikowski, A. P., Identification of HDAC6-Selective Inhibitors of Low Cancer Cell Cytotoxicity. *ChemMedChem* **2016,** *11* (1), 81-92.
26. Butler, K. V.; Kalin, J.; Brochier, C.; Vistoli, G.; Langley, B.; Kozikowski, A. P., Rational Design and Simple Chemistry Yield a Superior, Neuroprotective HDAC6 Inhibitor, Tubastatin A. *Journal of the American Chemical Society* **2010,** *132* (31), 10842-10846.
27. Bergman, J. A.; Woan, K.; Perez-Villarroel, P.; Villagra, A.; Sotomayor, E. M.; Kozikowski, A. P., Selective Histone Deacetylase 6 Inhibitors Bearing Substituted Urea Linkers Inhibit Melanoma Cell Growth. *Journal of Medicinal Chemistry* **2012,** *55* (22), 9891-9899.
28. Senger, J.; Melesina, J.; Marek, M.; Romier, C.; Oehme, I.; Witt, O.; Sippl, W.; Jung, M., Synthesis and Biological Investigation of Oxazole Hydroxamates as Highly Selective Histone Deacetylase 6 (HDAC6) Inhibitors. *Journal of Medicinal Chemistry* **2016,** *59* (4), 1545-1555.
29. Lee, J. H.; Mahendran, A.; Yao, Y.; Ngo, L.; Venta-Perez, G.; Choy, M. L.; Kim, N.; Ham, W. S.; Breslow, R.; Marks, P. A., Development of a histone deacetylase 6 inhibitor and its biological effects. *Proc Natl Acad Sci U S A* **2013,** *110* (39), 15704-9.
30. Kozikowski, A. P.; Tapadar, S.; Luchini, D. N.; Kim, K. H.; Billadeau, D. D., Use of the Nitrile Oxide Cycloaddition (NOC) Reaction for Molecular Probe Generation: A New Class of Enzyme Selective Histone Deacetylase Inhibitors (HDACIs) Showing Picomolar Activity at HDAC6. *Journal of Medicinal Chemistry* **2008,** *51* (15), 4370-4373.

31. Finnin, M. S.; Donigian, J. R.; Cohen, A.; Richon, V. M.; Rifkind, R. A.; Marks, P. A.; Breslow, R.; Pavletich, N. P., Structures of a histone deacetylase homologue bound to the TSA and SAHA inhibitors. *Nature* **1999,** *401*, 188.
32. Estiu, G.; Greenberg, E.; Harrison, C. B.; Kwiatkowski, N. P.; Mazitschek, R.; Bradner, J. E.; Wiest, O., Structural origin of selectivity in class II-selective histone deacetylase inhibitors. *Journal of medicinal chemistry* **2008,** *51* (10), 2898-2906.
33. Bieliauskas, A. V.; Pflum, M. K., Isoform-selective histone deacetylase inhibitors. *Chemical Society Reviews* **2008,** *37* (7), 1402-13.
34. Fleming, C. L.; Ashton, T. D.; Gaur, V.; McGee, S. L.; Pfeffer, F. M., Improved Synthesis and Structural Reassignment of MC1568: A Class IIa Selective HDAC Inhibitor. *Journal of Medicinal Chemistry* **2014,** *57* (3), 1132-1135.
35. Negmeldin, A. T.; Knoff, J. R.; Pflum, M. K. H., The structural requirements of histone deacetylase inhibitors: C4-modified SAHA analogs display dual HDAC6/HDAC8 selectivity. *European Journal of Medicinal Chemistry* **2018,** *143*, 1790-1806.
36. Yang, Z.; Wang, T.; Wang, F.; Niu, T.; Liu, Z.; Chen, X.; Long, C.; Tang, M.; Cao, D.; Wang, X.; Xiang, W.; Yi, Y.; Ma, L.; You, J.; Chen, L., Discovery of Selective Histone Deacetylase 6 Inhibitors Using the Quinazoline as the Cap for the Treatment of Cancer. *J Med Chem* **2016,** *59* (4), 1455-70.
37. Lee, J.-H.; Yao, Y.; Mahendran, A.; Ngo, L.; Venta-Perez, G.; Choy, M. L.; Breslow, R.; Marks, P. A., Creation of a histone deacetylase 6 inhibitor and its biological effects. *Proceedings of the National Academy of Sciences* **2015,** *112* (39), 12005-12010.
38. Kaliszczak, M.; Trousil, S.; Aberg, O.; Perumal, M.; Nguyen, Q. D.; Aboagye, E. O., A novel small molecule hydroxamate preferentially inhibits HDAC6 activity and tumour growth. *Br J Cancer* **2013,** *108* (2), 342-50.
39. North, B. J.; Almeciga-Pinto, I.; Tamang, D.; Yang, M.; Jones, S. S.; Quayle, S. N., Enhancement of pomalidomide anti-tumor response with ACY-241, a selective HDAC6 inhibitor. *PLOS ONE* **2017,** *12* (3), e0173507.
40. Hideshima, T.; Qi, J.; Paranal, R. M.; Tang, W.; Greenberg, E.; West, N.; Colling, M. E.; Estiu, G.; Mazitschek, R.; Perry, J. A.; Ohguchi, H.; Cottini, F.; Mimura, N.; Gorgun, G.; Tai, Y. T.; Richardson, P. G.; Carrasco, R. D.; Wiest, O.; Schreiber, S. L.; Anderson, K. C.; Bradner, J. E., Discovery of selective small-molecule HDAC6 inhibitor for overcoming proteasome inhibitor resistance in multiple myeloma. *Proc Natl Acad Sci U S A* **2016,** *113* (46), 13162-13167.
41. Namdar, M.; Perez, G.; Ngo, L.; Marks, P. A., Selective inhibition of histone deacetylase 6 (HDAC6) induces DNA damage and sensitizes transformed cells to anticancer agents. *Proceedings of the National Academy of Sciences* **2010,** *107* (46), 20003-20008.
42. Vogl, D. T.; Raje, N.; Jagannath, S.; Richardson, P.; Hari, P.; Orlowski, R.; Supko, J. G.; Tamang, D.; Yang, M.; Jones, S. S.; Wheeler, C.; Markelewicz, R. J.; Lonial, S., Ricolinostat, the First Selective Histone Deacetylase 6 Inhibitor, in Combination with Bortezomib and Dexamethasone for Relapsed or Refractory Multiple Myeloma. *Clinical Cancer Research* **2017,** *23* (13), 3307-3315.
43. Gerova, M. S.; Petrov, O. I., A Convenient Synthesis of the New Histone Deacetylase Inhibitor Scriptaid. *Organic Preparations and Procedures International* **2014,** *46* (1), 76-79.
44. Su, G. H.; Sohn, T. A.; Ryu, B.; Kern, S. E., A Novel Histone Deacetylase Inhibitor Identified by High-Throughput Transcriptional Screening of a Compound Library. *Cancer Res.* **2000,** *60*, 3137-3142.
45. Wang, G.; Jiang, X.; Pu, H.; Zhang, W.; An, C.; Hu, X.; Liou, A. K.; Leak, R. K.; Gao, Y.; Chen, J., Scriptaid, a novel histone deacetylase inhibitor, protects against traumatic brain injury via modulation of PTEN and AKT pathway : scriptaid protects against TBI via AKT. *Neurotherapeutics* **2013,** *10* (1), 124-42.
46. Ying, H.; Zhang, Y.; Lin, S.; Han, Y.; Zhu, H.-Z., Histone deacetylase inhibitor Scriptaid reactivates latent HIV-1 promoter by inducing histone modification in in vitro latency cell lines. *International Journal of Molecular Medicine* **2010,** *26* (2), 265-272.
47. Gaur, V.; Connor, T.; Sanigorski, A.; Martin, Sheree D.; Bruce, Clinton R.; Henstridge, Darren C.; Bond, Simon T.; McEwen, Kevin A.; Kerr-Bayles, L.; Ashton, Trent D.; Fleming, C.; Wu, M.; Pike Winer, Lisa S.; Chen, D.; Hudson, Gregg M.; Schwabe, John W. R.; Baar, K.; Febbraio, Mark A.; Gregorevic, P.; Pfeffer, Frederick M.; Walder, Ken R.; Hargreaves, M.; McGee, Sean L., Disruption of the Class IIa HDAC Corepressor Complex Increases Energy Expenditure and Lipid Oxidation. *Cell Reports* **2016,** *16* (11), 2802-2810.
48. Rivieccio, M. A.; Brochier, C.; Willis, D. E.; Walker, B. A.; D'Annibale, M. A.; McLaughlin, K.; Siddiq, A.; Kozikowski, A. P.; Jaffrey, S. R.; Twiss, J. L.; Ratan, R. R.; Langley, B., HDAC6 is a target for protection and regeneration following injury in the nervous system. *Proceedings of the National Academy of Sciences* **2009,** *106* (46), 19599-19604.

49. Shi, P.; Scott, M. A.; Ghosh, B.; Wan, D.; Wissner-Gross, Z.; Mazitschek, R.; Haggarty, S. J.; Yanik, M. F., Synapse microarray identification of small molecules that enhance synaptogenesis. *Nat Commun* **2011,** *2*, 510.

50. Fleming, C. L.; Ashton, T. D.; Nowell, C.; Devlin, M.; Natoli, A.; Schreuders, J.; Pfeffer, F. M., A fluorescent histone deacetylase (HDAC) inhibitor for cellular imaging. *Chemical Communications* **2015,** *51* (37), 7827-7830.

51. Keen, J. C.; Yan, L.; Mack, K. M.; Pettit, C.; Smith, D.; Sharma, D.; Davidson, N. E., A novel histone deacetylase inhibitor, Scriptaid, enhances expression of functional estrogen receptor α (ER) in ER negative human breast cancer cells in combination with 5-aza 2'-deoxycytidine. *Breast Cancer Research and Treatment* **2003,** *81*, 177-186.

52. Giacinti, L.; Giacinti, C.; Gabellini, C.; Rizzuto, E.; Lopez, M.; Giordano, A., Scriptaid effects on breast cancer cell lines. *J Cell Physiol* **2012,** *227* (10), 3426-33.

53. Gillet, N.; Vandermeers, F.; de Brogniez, A.; Florins, A.; Nigro, A.; Francois, C.; Bouzar, A. B.; Verlaeten, O.; Stern, E.; Lambert, D. M.; Wouters, J.; Willems, L., Chemoresistance to Valproate Treatment of Bovine Leukemia Virus-Infected Sheep; Identification of Improved HDAC Inhibitors. *Pathogens* **2012,** *1* (2), 65-82.

54. Pasini, A.; Marchetti, C.; Sissi, C.; Cortesi, M.; Giordano, E.; Minarini, A.; Milelli, A., Novel Polyamine–Naphthalene Diimide Conjugates Targeting Histone Deacetylases and DNA for Cancer Phenotype Reprogramming. *ACS Medicinal Chemistry Letters* **2017,** *8* (12), 1218-1223.

55. Vaisburg, A.; Bernstein, N.; Frechette, S.; Allan, M.; Abou-Khalil, E.; Leit, S.; Moradei, O.; Bouchain, G.; Wang, J.; Woo, S. H.; Fournel, M.; Yan, P. T.; Trachy-Bourget, M.-C.; Kalita, A.; Beaulieu, C.; Li, Z.; MacLeod, A. R.; Besterman, J. M.; Delorme, D., (2-Amino-phenyl)-amides of ω-substituted alkanoic acids as new histone deacetylase inhibitors. *Bioorganic & Medicinal Chemistry Letters* **2004,** *14* (1), 283-287.

56. Wong, J. C.; Hong, R.; Schreiber, S. L., Structural Biasing Elements for In-Cell Histone Deacetylase Paralog Selectivity. *Journal of the American Chemical Society* **2003,** *125* (19), 5586-5587.

57. Zhang, Y.; Yan, J.; Yao, T.-P., Discovery of a fluorescent probe with HDAC6 selective inhibition. *European Journal of Medicinal Chemistry* **2017,** *141*, 596-602.

58. Kolanowski, J. L.; Liu, F.; New, E. J., Fluorescent probes for the simultaneous detection of multiple analytes in biology. *Chemical Society Reviews* **2018,** *47* (1), 195-208.

59. New, E. J., Harnessing the Potential of Small Molecule Intracellular Fluorescent Sensors. *ACS Sensors* **2016,** *1* (4), 328-333.

60. Ashton, T. D.; Jolliffe, K. A.; Pfeffer, F. M., Luminescent probes for the bioimaging of small anionic species in vitro and in vivo. *Chemical Society Reviews* **2015,** *44* (14), 4547-4595.

61. He, X.-P.; Tian, H., Lightening Up Membrane Receptors with Fluorescent Molecular Probes and Supramolecular Materials. *Chem 4* (2), 246-268.

62. Poynton, F. E.; Bright, S. A.; Blasco, S.; Williams, D. C.; Kelly, J. M.; Gunnlaugsson, T., The development of ruthenium(ii) polypyridyl complexes and conjugates for in vitro cellular and in vivo applications. *Chemical Society Reviews* **2017,** *46* (24), 7706-7756.

63. Aulsebrook, M. L.; Graham, B.; Grace, M. R.; Tuck, K. L., Lanthanide complexes for luminescence-based sensing of low molecular weight analytes. *Coordination Chemistry Reviews* **2017**.

64. Surender, Esther M.; Comby, S.; Cavanagh, B. L.; Brennan, O.; Lee, T. C.; Gunnlaugsson, T., Two-Photon Luminescent Bone Imaging Using Europium Nanoagents. *Chem 1* (3), 438-455.

65. Yenugonda, V. M.; Deb, T. B.; Grindrod, S. C.; Dakshanamurthy, S.; Yang, Y.; Paige, M.; Brown, M. L., Fluorescent cyclin-dependent kinase inhibitors block the proliferation of human breast cancer cells. *Bioorganic & Medicinal Chemistry* **2011,** *19* (8), 2714-2725.

66. Kong, Y.; Jung, M.; Wang, K.; Grindrod, S.; Velena, A.; Lee, S. A.; Dakshanamurthy, S.; Yang, Y.; Miessau, M.; Zheng, C.; Dritschilo, A.; Brown, M. L., Histone deacetylase cytoplasmic trapping by a novel fluorescent HDAC inhibitor. *Mol Cancer Ther* **2011,** *10* (9), 1591-9.

67. Barbara, C.; Ewelina, S.; Robert, M., Quinoline Fluorescent Probes for Zinc – from Diagnostic to Therapeutic Molecules in Treating Neurodegenerative Diseases. *Medicinal Chemistry* **2018,** *14* (1), 19-33.

68. Qian, J.; Tang, B. Z., AIE Luminogens for Bioimaging and Theranostics: From Organelles to Animals. *Chem 3* (1), 56-91.

69. Lee, M. H.; Sharma, A.; Chang, M. J.; Lee, J.; Son, S.; Sessler, J. L.; Kang, C.; Kim, J. S., Fluorogenic reaction-based prodrug conjugates as targeted cancer theranostics. *Chemical Society Reviews* **2018,** *47* (1), 28-52.

70. Meng, Q.; Liu, Z.; Li, F.; Ma, J.; Wang, H.; Huan, Y.; Li, Z., An HDAC-Targeted Imaging Probe LBH589–Cy5.5 for Tumor Detection and Therapy Evaluation. *Molecular Pharmaceutics* **2015,** *12* (7), 2469-2476.

71. Ye, R. R.; Ke, Z. F.; Tan, C. P.; He, L.; Ji, L. N.; Mao, Z. W., Histone-deacetylase-targeted fluorescent ruthenium(II) polypyridyl complexes as potent anticancer agents. *Chemistry* **2013,** *19* (31), 10160-9.
72. Singh, R. K.; Mandal, T.; Balasubramanian, N.; Cook, G.; Srivastava, D. K., Coumarin-suberoylanilide hydroxamic acid as a fluorescent probe for determining binding affinities and off-rates of histone deacetylase inhibitors. *Analytical Biochemistry* **2011,** *408* (2), 309-315.
73. Kindahl, T.; Chorell, E.; Chorell, E., Development and Optimization of Simple One-Step Methods for the Synthesis of 4-Amino-Substituted 1,8-Naphthalimides. *European Journal of Organic Chemistry* **2014,** *2014* (28), 6175-6182.
74. Fleming, C. L.; Ashton, T. D.; Pfeffer, F. M., Synthesis of 4-amino substituted 1,8-naphthalimide derivatives using palladium-mediated amination. *Dyes and Pigments* **2014,** *109*, 135-143.
75. Hearn, K. N.; Nalder, T. D.; Cox, R. P.; Maynard, H. D.; Bell, T. D. M.; Pfeffer, F. M.; Ashton, T. D., Modular synthesis of 4-aminocarbonyl substituted 1,8-naphthalimides and application in single molecule fluorescence detection. *Chemical Communications* **2017,** *53* (91), 12298-12301.
76. Hai, Y.; Christianson, D. W., Histone deacetylase 6 structure and molecular basis of catalysis and inhibition. *Nature Chemical Biology* **2016,** *12*, 741.
77. Bao, X.; Wu, X.; Berry, S. N.; Howe, E. N. W.; Chang, Y.-T.; Gale, P. A., Fluorescent squaramides as anion receptors and transmembrane anion transporters. *Chemical Communications* **2018,** *54* (11), 1363-1366.
78. Leslie, K.; Jacquemin, D.; New, E.; Jolliffe, K., Expanding the breadth of 4-amino-1,8-naphthalimide photophysical properties through substitution of the naphthalimide core. *Chemistry – A European Journal* **2018,** *24* (21), 5569-5573.
79. Duke, R. M.; Veale, E. B.; Pfeffer, F. M.; Kruger, P. E.; Gunnlaugsson, T., Colorimetric and fluorescent anion sensors: an overview of recent developments in the use of 1,8-naphthalimide-based chemosensors. *Chemical Society Reviews* **2010,** *39* (10), 3936-3953.
80. Zheng, S.; Lynch, P. L. M.; Rice, T. E.; Moody, T. S.; Gunaratne, H. Q. N.; de Silva, A. P., Structural effects on the pH-dependent fluorescence of naphthalenic derivatives and consequences for sensing/switching. *Photochemical & Photobiological Sciences* **2012,** *11* (11), 1675-1681.
81. Kazmi, F.; Hensley, T.; Pope, C.; Funk, R. S.; Loewen, G. J.; Buckley, D. B.; Parkinson, A., Lysosomal Sequestration (Trapping) of Lipophilic Amine (Cationic Amphiphilic) Drugs in Immortalized Human Hepatocytes (Fa2N-4 Cells). *Drug Metabolism and Disposition* **2013,** *41* (4), 897-905.
82. Peterson, R. T.; MacRae, C. A., Systematic Approaches to Toxicology in the Zebrafish. *Annual Review of Pharmacology and Toxicology* **2012,** *52* (1), 433-453.
83. Jobe, K.; Brennan, C. H.; Motevalli, M.; Goldup, S. M.; Watkinson, M., Modular 'click' sensors for zinc and their application in vivo. *Chem Commun (Camb)* **2011,** *47* (21), 6036-8.
84. Pancholi, J.; Hodson, D. J.; Jobe, K.; Rutter, G. A.; Goldup, S. M.; Watkinson, M., Biologically targeted probes for Zn(2+): a diversity oriented modular "click-SNAr-click" approach *Chem Sci* **2014,** *5* (9), 3528-3535.
85. Li, L.; Bonneton, F.; Tohme, M.; Bernard, L.; Chen, X. Y.; Laudet, V., In Vivo Screening Using Transgenic Zebrafish Embryos Reveals New Effects of HDAC Inhibitors Trichostatin A and Valproic Acid on Organogenesis. *PLoS One* **2016,** *11* (2), e0149497.
86. Habeck, H.; Odenthal, J.; Walderich, B.; Maischein, H.-M.; Schulte-Merker, S., Analysis of a Zebrafish VEGF Receptor Mutant Reveals Specific Disruption of Angiogenesis. *Current Biology* **2002,** *12* (16), 1405-1412.
87. Bradner, J. E.; West, N.; Grachan, M. L.; Greenberg, E. F.; Haggarty, S. J.; Warnow, T.; Mazitschek, R., Chemical phylogenetics of histone deacetylases. *Nature Chemical Biology* **2010,** *6*, 238.
88. Huber, K.; Doyon, G.; Plaks, J.; Fyne, E.; Mellors, J. W.; Sluis-Cremer, N., Inhibitors of Histone Deacetylases: Correlation Between Isoform Specificity and Reactivation of HIV Type 1 (HIV-1) From Latently Infected Cells. *Journal of Biological Chemistry* **2011,** *286* (25), 22211-22218.

Highlights:

- New highly fluorescent HDAC inhibitors based on scriptaid.
- Low-nanomolar activity against HDAC6 and more than 500-fold selectivity for HDAC6 over HDAC1.
- Imaging studies show uptake and localisation in cellular cytoplasm and zebrafish vasculature.
- The selective HDAC6 inhibition leads to a mild phenotypical outcome in zebrafish